The American Journal of Pathology, Vol. 181, No. 6, December 2012

http://dx.doi.org/10.1016/j.ajpath.2012.08.038

Gastrointestinal, Hepatobiliary, and Pancreatic Pathology

Pancreatic STAT3 Protects Mice against Caerulein-Induced Pancreatitis via PAP1 Induction

Minoru Shigekawa,* Hayato Hikita,* Takahiro Kodama,* Satoshi Shimizu,* Wei Li,* Akio Uemura,* Takuya Miyagi,* Atsushi Hosui,* Tatsuya Kanto,* Naoki Hiramatsu,* Tomohide Tatsumi,* Kiyoshi Takeda,† Shizuo Akira,‡ and Tetsuo Takehara*

From the Department of Gastroenterology and Hepatology and the Laboratory of Immune Regulation,† Department of Microbiology and Immunology, Osaka University Graduated School of Medicine, Suita; and the Laboratory of Host Defense,‡ World Premier International Immunology Frontier Research Center, Suita, Japan*

The signal transducer and activator of transcription 3 (STAT3) is a transcription factor that controls expressions of several genes involved in cell survival, proliferation and differentiation, and tissue inflammation. However, the significance of pancreatic STAT3 in acute pancreatitis remains unclear. We generated conditional STAT3 knockout ($stat3^{\Delta/\Delta}$) mice by crossing $stat3^{flox/flox}$ mice with Pdx1-promoter Cre transgenic mice. Caerulein administration activated pancreatic STAT3 and induced acute pancreatitis as early as 3 hours in wild-type mice, and full recovery from the induced pancreatic injury was observed within 7 days. The levels of serum amylase and lipase and histologic scores of pancreatic necrosis and inflammatory cell infiltration were significantly higher at 3 hours in $stat3^{\Delta/\Delta}$ mice than in $stat3^{flox/flox}$ mice. Pancreatic recovery after pancreatitis was significantly delayed in $stat3^{\Delta/\Delta}$ mice compared with $stat3^{flox/flox}$ mice. Although $stat3^{flox/flox}$ mice had marked production in the pancreas of pancreatitis-associated protein 1 (PAP1), a serum acute phase protein, this induction was completely abrogated in $stat3^{\Delta/\Delta}$ mice. Enforced production of PAP1 by a hydrodynamic procedure in the liver significantly suppressed pancreatic necrosis and inflammation and also promoted pancreatic regeneration and recovery in $stat3^{\Delta/\Delta}$ mice to levels similar to those observed in $stat3^{flox/flox}$ mice. In conclusion, pancreatic STAT3 is indispensable for PAP1 production, and this STAT3/PAP1 pathway plays a protective role in caerulein-induced pancreatitis. (Am J Pathol 2012, 181:2105–2113; http://dx.doi.org/10.1016/j.ajpath.2012.08.038)

Acute pancreatitis is a common digestive disease characterized by edema, necrosis, hemorrhage, and severe inflammatory cell infiltration of the pancreas.[1] Its onset is triggered by acinar events, involving premature intra-acinar activation of digestive zymogens that induce autodigestion and acinar cell injury.[2] Previous studies have reported that cytokines, especially proinflammatory cytokines, such as tumor necrosis factor (TNF)-α, IL-1β and IL-6, and chemokines [eg, monocyte chemoattractant protein-1 (MCP-1)] derived from stimulated acinar cells, play a key role in the disease pathology of acute pancreatitis.[3] Acinar cell destruction also results in activation and infiltration of inflammatory cells, which release proinflammatory mediators, such as the cytokines and reactive oxygen species.[4] Excessive production of cytokines leads to a systemic inflammatory response and multiple organ failure,[5] as evidenced by the fact that levels of circulating inflammatory cytokines, including IL-6, are correlated with disease severity in human pancreatitis.[6–8] Acute pancreatitis remains a difficult clinical problem, causing severe motility and morbidity. Thus, the cellular mechanisms underlying the pathogenesis of acute pancreatitis need to be elucidated.

The signal transducers and activators of the transcription (STAT) family are transcription factors that are associated with mediating inflammatory responses. The STAT signaling pathway is activated by a diverse array of cytokines and growth factors and has been implicated in a variety of biological events, such as proliferation, cell survival, and immune response.[9] Among the STAT family, STAT3 was formerly known as an acute-phase response factor, which regulates the expression of genes involved in a series of inflammatory reactions induced in response to infection and tissue injury.[10] Proinflammatory cytokine IL-6[11] or lipopolysaccharides[12] have been shown to activate this factor. Previous reports indicate that STAT3 protects cardiomyocytes against apoptosis during myocardiac injury[13] and promotes proliferation in hepatocytes after partial hepatectomy.[14] In

Supported by a Grant-in-Aid for Scientific Research from the Ministry of Education, Culture, Sports, Science, and Technology, Japan.

Accepted for publication August 28, 2012.

Supplemental material for this article can be found at *http://ajp.amjpathol.org* or at *http://dx.doi.org/10.1016/j.ajpath.2012.08.038*.

Address reprint requests to Tetsuo Takehara, M.D., Ph.D., 2-2 Yamada-oka, Suita, Osaka 565-0871, Japan. E-mail: takehara@gh.med.osaka-u.ac.jp.

addition, we have previously demonstrated that the soluble factors dependent on hepatic STAT3, such as acute-phase proteins, suppress innate immune cell overactivation and hypercytokinemia to aid host defense during systemic inflammation.[15] Recent studies have found that STAT3 in acinar cells could be activated by several inflammatory mediators, such as TNF-α or lipopolysaccharide.[16,17] In addition, STAT3 activated by oxidative stress was found to induce MCP-1 expression in acinar cells.[18] Although this transcription factor may be involved in pancreatic injury during acute inflammation, the pathologic and physiologic mechanisms of pancreatitis in relation to the pancreatic STAT3 pathway remain unclear.

In the present study, we examined the effects of the pancreatic STAT3 signaling pathway on acute pancreatitis. Because systemic deletion of STAT3 leads to embryonic lethality in mice,[19] we used conditional knockout mice with deletion of pancreatic STAT3 using the Cre/loxP system. We found that its signaling pathway offered protection from acinar cell death and inflammatory cell infiltration during caerulein-induced pancreatitis. Moreover, the expression of pancreatitis-associated protein 1 (PAP1) from the pancreas, which is known as an acute-phase response factor in inflammation, was completely dependent on pancreatic STAT3 and was involved in attenuation of the severity of pancreatitis in mice with deletion of pancreatic STAT3. Thus, we concluded that pancreatic STAT3 plays a protective role in modulating pancreatic injury and inflammatory infiltration during caerulein-induced pancreatitis via PAP1 production.

Materials and Methods

Animals

Mice carrying a *STAT3* gene with 2 loxP sequences flanking exon 22 (*stat3*$^{flox/flox}$) have been described previously.[20] Conditional STAT3 knockout (*stat3*$^{\Delta/\Delta}$) mice were generated by crossing *stat3*$^{flox/flox}$ mice with *pdx1-Cre* transgenic mice to obtain deletion of STAT3 within the pancreas. Sex-matched *stat3*$^{flox/flox}$ mice obtained from the same litter were used as wild-type (WT) controls. All animals were used at the age of 7 to 10 weeks and housed with 12-hour light/dark cycles with free access to food and water under specific pathogen-free conditions. Mice were treated with humane care under approval from the Animal Care and Use Committee of Osaka University Medical School.

Animal Model of Acute Pancreatitis

Acute pancreatitis was induced by eight hourly i.p. injections of 50 μg/kg of caerulein (Sigma-Aldrich, St. Louis, MO) for 2 consecutive days, whereas the controls were administered PBS in the same way. For caerulein-induced pancreatitis, *stat3*$^{\Delta/\Delta}$ and *stat3*$^{flox/flox}$ mice were fasted for 12 hours before the treatment but provided with water *ad libitum*.

Preparation of Tissue and Serum Samples

Tissues from the pancreas were removed, weighed, immediately frozen in liquid nitrogen, and stored at −80°C. Myeloperoxidase activity in the pancreas samples was measured using a Myeloperoxidase Detection Kit according to the manufacturer's protocol (Cell Technology Inc., Mountain View, CA). Whole blood samples were centrifuged at 15,000 × *g* for 20 minutes at 20°C, and serum was used for biochemical examinations of amylase and lipase with commercially available assays (Nagahama Life Science Laboratory, Nagahama, Japan).

Histologic Analysis

Formalin-fixed pancreatic tissue sections were stained with H&E to assess pancreatic necrosis and inflammatory cell infiltration. Necrotic cells were defined as ones that were swollen, had lost plasma membrane integrity, and had leakage of cytoplasm into the interstitium. The extent of the necrotic area was scored using the following scale: 0, none; 1, <30%; 2, 30% to 70%; and 3, >70%. Quantification of the necrotic area (necrotic area score) was the sum of the scales obtained in four high-powered fields of pancreatic tissue sections with H&E on a range of 0 to 12. In a similar way, the intensity of inflammatory infiltration (inflammatory infiltration score) was scored in four fields, using the following 1- to 3-point scale (resulting in a score of 0 to 12) for the extension of inflammatory cell infiltration: 0, none; 1, surrounding pancreas; 2, intralobular area; and 3, surrounding acini. To detect apoptotic cells, the pancreatic tissue sections were also subjected to TUNEL staining as previously reported.[21] To assess proliferative cells in the injured pancreas, pancreatic sections were stained using an anti–Ki-67 antibody (Abcam, Cambridge, MA).

Western Blot Analysis

Approximately 25 mg of pancreatic tissues was lysed with a lysis buffer [1% NP-40, 0.5% sodium deoxycholate, 0.1% sodium dodecyl sulfate, 1× protease inhibitor cocktail (Nacalai Tesque, Kyoto, Japan), 1× phosphatase inhibitor cocktail (Nacalai Tesque), and phosphate-buffered saline (pH 7.4)]. After incubation on ice for 20 minutes, the lysate was centrifuged at 10,000 × *g* for 20 minutes at 4°C. The protein content of the supernatant was determined using a bicinchoninic acid protein assay kit (Pierce, Rockford, IL). Equal amounts of protein were electrophoretically separated by SDS-PAGE and transferred onto polyvinylidene fluoride membrane. For immunodetection, the following antibodies were used: anti–phospho-STAT3 (Tyr705) antibody, anti-STAT3 antibody (Cell Signaling Technology, Danvers, MA), anti–Bcl-xL antibody (Santa Cruz Biotechnology Inc, Delaware, CA), anti–Mcl-1 antibody (Rockland, Gilbertsville, PA), anti–β-actin antibody (Sigma-Aldrich), and anti-mouse RegIIIB (PAP1) antibody (R&D Systems, Minneapolis, MN).

Real-Time RT-PCR

Total RNA was extracted from the pancreatic tissue using an RNeasy kit (QIAGEN, Tokyo, Japan). For complementary DNA synthesis, 1 μg of total RNA was reverse transcribed using the High Capacity RNA-to-DNA Master Mix

(Applied Biosystems Inc, Foster City, CA) and subjected to real-time RT-PCR. The mRNA expression of specific genes was measured using Taqman Gene Expression Assays (Applied Biosystems Inc). Assay IDs of the respective genes are *Cd68*: Mm03047343_m1, *il6*: Mm01210733_m1, and *Ccl2*: Mm00441242_m1.The levels of gene expression were corrected with the quantified expression level of glyceraldehyde 3-phosphate dehydrogenase (*Gapdh*: Mm99999915_g1) mRNA.

Enzyme-Linked Immunosorbent Assay

The levels of IL-6 in serum were measured using Quantikine Mouse IL-6 Immunoassay (R&D Systems) according to the manufacturer's protocol.

Injection of Naked Plasmid DNA

A plasmid containing the murine full-length *Reg3A* (human alias, *PAP1*) gene (pCMV-PAP1; C-terminal Myc and DDK tagged) was purchased from Origene Technologies Inc (Rockville, MD). The plasmid itself served as a control (pCMV). The plasmid DNA was prepared using an EndoFree plasmid system (QIAGEN) according to the manufacturer's instructions. Hydrodynamic injection of plasmid DNA was performed as previously described.[22] In brief, 50 μg of plasmid DNA was diluted with 2.0 mL of lactated Ringer's solution and injected into the tail vein, using a syringe with a 26-gauge needle. DNA injection was completed within 5 to 8 seconds.

Statistical Analysis

Data are presented as the mean ± SD. Differences between groups were compared using the unpaired *t*-test. The level of statistical significance was set at $P < 0.05$.

Results

Pancreatic STAT3 Is Activated in the Early Phase of Pancreatitis

Acute pancreatitis was induced by repetitive i.p. injections of caerulein, an analog of the secretagogue cholecystokinin, to WT mice, and activation of STAT3 was observed in the pancreas. Western blot analysis clearly revealed phosphorylation of STAT3 in the pancreas at 3, 24, and 72 hours after the last injection of caerulein; expression was strongest at 3 hours and decreased over time (Figure 1A). WT mice given caerulein treatment had a significant increase in serum levels of amylase at 3 hours but not at later time points (Figure 1B). Histologic findings at 3 hours revealed typical morphologic changes characterized by edema, vacuolization, inflammatory cell infiltration, and acinar cell death, which were gradually improved at later time points (Figure 1C). We evaluated

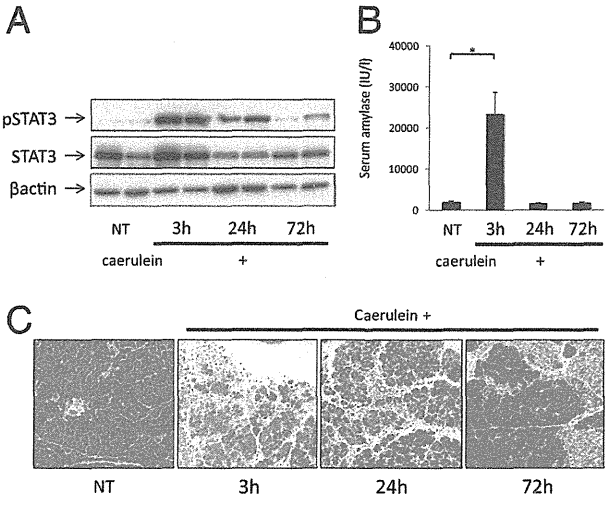

Figure 1. Activation of pancreatic STAT3 in caerulein-induced pancreatitis. WT mice were subjected to eight hourly i.p. injections of caerulein (50 μg/kg) for 2 consecutive days. The mice were sacrificed at 3, 24, or 72 hours after the last injection ($n = 8$ per group). The mice without caerulein treatment (NT) served as controls. **A:** Expressions of STAT3 and phosphorylated STAT3 (pSTAT3) in the pancreas were assessed by Western blot analysis. β-Actin was included as a control. **B:** Pancreatic injury was determined by measuring serum levels of amylase. $^*P < 0.05$. **C:** Representative views of H&E staining of the pancreatic sections. Original magnification, ×200.

the function of pancreatic STAT3 during caerulein-induced pancreatitis, mainly 3 hours after the last injection.

Ablation of Pancreatic STAT3 Exacerbates Caerulein-Induced Pancreatitis

Conditional STAT3 knockout mice were generated by crossing floxed STAT3 mice and *pdx1-Cre* transgenic mice. *Pdx1* is known to be expressed in the developing pancreas, stomach, and duodenum of mice.[23] *stat3*$^{flox/flox}$ *pdx1-Cre* (ie, *stat3*$^{\Delta/\Delta}$) mice were born with the expected mendelian characteristics. No significant difference was found between body weight and serum levels of amylase and lipase between *stat3*$^{\Delta/\Delta}$ mice and *stat3*$^{flox/flox}$ mice at the age of 8 weeks (see Supplemental Figure S1, A and B, at *http://ajp.amjpathol.org*). The relative weight and histology of the pancreas also showed no difference between them (see Supplemental Figure S1, C and D, at *http://ajp.amjpathol.org*). As expected, *stat3*$^{\Delta/\Delta}$ pancreas expressed substantially lower levels of STAT3 than *stat3*$^{flox/flox}$ pancreas (Figure 2A). To clarify the significance of pancreatic STAT3 during acute pancreatitis, we examined the severities of caerulein-induced pancreatitis in *stat3*$^{\Delta/\Delta}$ and *stat3*$^{flox/flox}$ mice. In *stat3*$^{\Delta/\Delta}$ mice with caerulein treatment, serum levels of amylase and lipase were significantly higher than in *stat3*$^{flox/flox}$ mice at 3 hours after the last injection (Figure 2B). Histologic examination of *stat3*$^{\Delta/\Delta}$ pancreas revealed marked exacerbation of necrotic cell death and inflammatory cell infiltration compared with *stat3*$^{flox/flox}$ pancreas (Figure 2C). To detect apoptotic cells, the pancreatic sections were subjected to TUNEL staining. The number of TUNEL-positive cells was significantly higher at 3 hours after the last injection in *stat3*$^{\Delta/\Delta}$ pancreas than

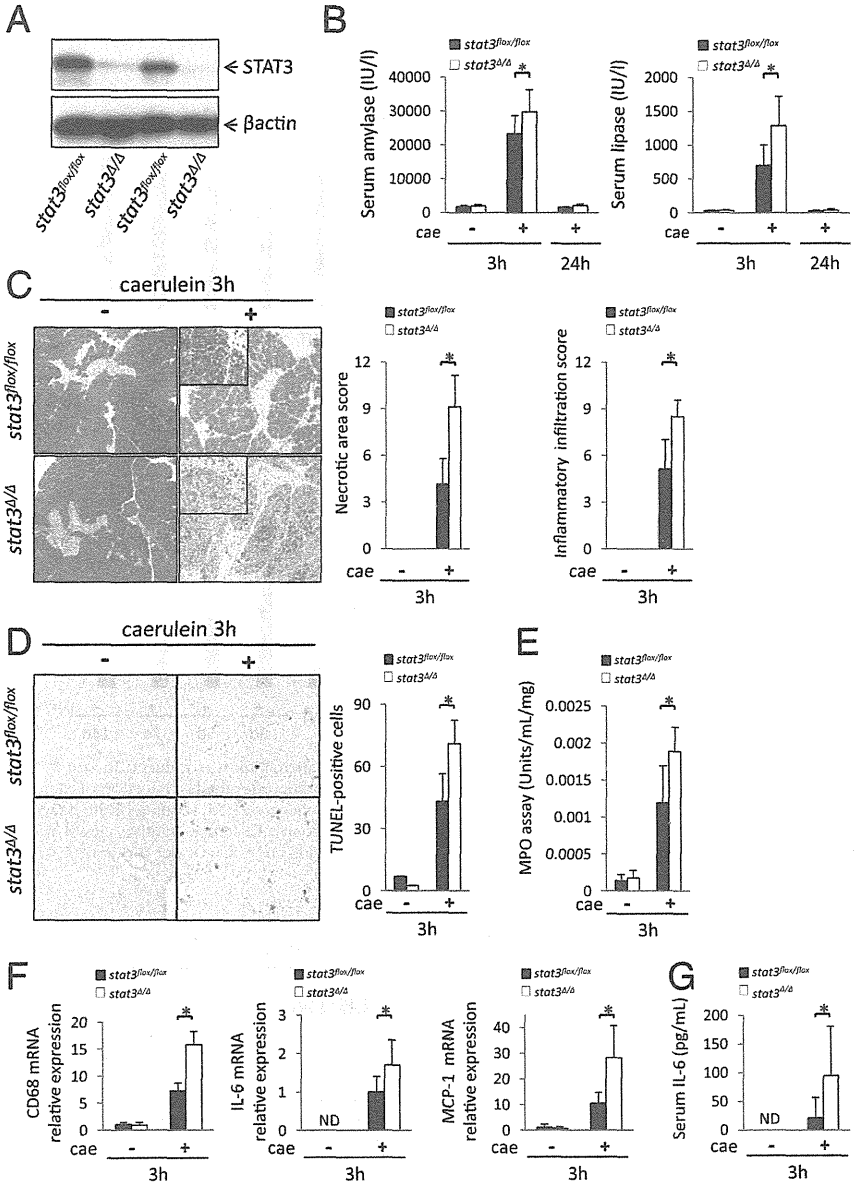

Figure 2. STAT3 knockdown in the pancreas increases caerulein-induced pancreatic injury. Acute pancreatitis was induced in *stat3*$^{\Delta/\Delta}$ and *stat3*$^{flox/flox}$ mice by eight hourly i.p. injections of caerulein (cae +) or vehicle (cae −) for 2 consecutive days. The mice were sacrificed at 3 or 24 hours after the last injection of caerulein. *stat3*$^{\Delta/\Delta}$ stands for *stat3*$^{flox/flox}$ *pdx1-Cre*. **A:** Expression of STAT3 in the pancreas of *stat3*$^{\Delta/\Delta}$ and *stat3*$^{flox/flox}$ mice before the treatment by Western blot analysis. **B:** Pancreatic injury was determined by measuring serum levels of amylase and lipase (n = 8 per group). **C:** Representative views of H&E staining of the pancreatic sections at 3 hours after the last injection of caerulein. Necrotic area score and inflammatory infiltration score were quantified on H&E-stained pancreatic sections (n = 6 to 8 per group). **D:** Representative views of TUNEL staining of the pancreatic sections at 3 hours after the last injection of caerulein and statistics of TUNEL-positive cells per six high-powered fields (n = 8 per group). **E:** Pancreatic myeloperoxidase activity was measured in the pancreas (n = 6 to 8 per group). **F:** Expression of CD68, IL-6, and MCP-1 mRNAs in the pancreas was assessed by real-time RT-PCR analysis (n = 6 to 8 per group). **G:** Expression of IL-6 in serum was assessed by enzyme-linked immunosorbent assay (n = 6 to 8 per group). *$P < 0.05$. ND, not detected. Original magnification: ×200 (**C**and **D**); ×400 (**inset** in **C**).

in *stat3*$^{flox/flox}$ pancreas (Figure 2D). *stat3*$^{\Delta/\Delta}$ mice with caerulein treatment had significantly increased levels of myeloperoxidase activity, which represented the levels of polymorphonuclear leukocyte infiltration, and mRNA expression of CD68, which is a marker of macrophages (Figure 2, E and F). In *stat3*$^{\Delta/\Delta}$ mice, mRNA expressions of inflammatory mediators, such as IL-6 and MCP-1 in the pancreas and IL-6 levels in circulation, significantly increased compared with *stat3*$^{flox/flox}$ mice (Figure 2, F and G).

Pancreatic Recovery Is Delayed in stat3$^{\Delta/\Delta}$ *Mice during Caerulein-Induced Pancreatitis*

Caerulein-induced epithelial injury is recognized as a fully reversible process.[24] To assess the regeneration process in our model, we examined the relative pancreatic weight and histologic features in *stat3*$^{\Delta/\Delta}$ and *stat3*$^{flox/flox}$ mice during caerulein-induced pancreatitis over time. In *stat3*$^{flox/flox}$ mice, histologic examination revealed that injured acinar cells were almost fully restored at 7 days after caerulein administration (Figure 3A). In agreement with this, relative pancreatic weight, which decreased after caerulein administration, recovered to the baseline levels at this time point (Figure 3B). The number of cells positive for Ki-67 protein, a cellular marker for proliferation, revealed the greatest increase at 3 days in *stat3*$^{flox/flox}$ pancreas and gradually decreased over time (Figure 3, C and D). On the other hand, *stat3*$^{\Delta/\Delta}$ mice had histologic exacerbation of the pancreas compared with *stat3*$^{flox/flox}$ mice after caerulein administration (Figure 3A). The relative pancreatic weight of *stat3*$^{\Delta/\Delta}$ mice was significantly lower at 3, 5, and 7 days than that of *stat3*$^{flox/flox}$ mice and finally recovered to the baseline levels at 14 days (Figure 3B). In addition, we observed a peak delay of the number of

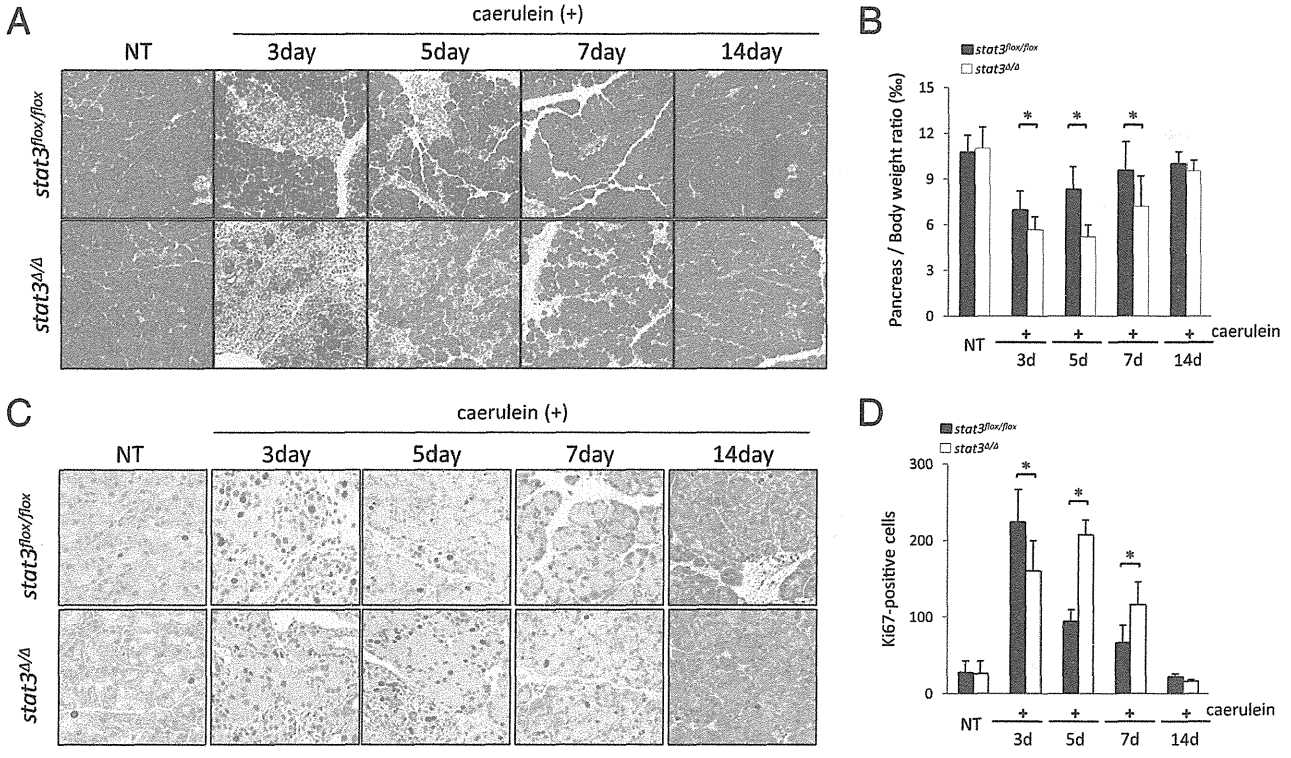

Figure 3. Delayed restoration of the injured pancreas in *stat3*$^{\Delta/\Delta}$ mice during caerulein-induced pancreatitis. Acute pancreatitis was induced in *stat3*$^{\Delta/\Delta}$ and *stat3*$^{flox/flox}$ mice by eight hourly i.p. injections of caerulein for 2 consecutive days. Mice were sacrificed at indicated time points after the last injection of caerulein. The mice without caerulein treatment (NT) served as controls. *stat3*$^{\Delta/\Delta}$ stands for *stat3*$^{flox/flox}$ *pdx1-Cre*. **A:** Representative views of H&E staining of the pancreatic sections in *stat3*$^{\Delta/\Delta}$ and *stat3*$^{flox/flox}$ mice. **B:** Relative pancreatic weight in *stat3*$^{\Delta/\Delta}$ and *stat3*$^{flox/flox}$ mice (n = 7 per group). **C:** Representative views of Ki-67 immunohistochemical staining of the pancreatic sections. **D:** Statistics of Ki-67-positive cells per four high-powered fields (n = 4 to 8 per group). *$P < 0.05$. Original magnification: ×200 (**A** and **C**).

Ki-67 positive cells in the pancreas of *stat3*$^{\Delta/\Delta}$ mice (Figure 3, C and D). A loss of pancreatic STAT3 led to delayed restoration of the injured pancreas during caerulein-induced pancreatitis.

PAP1 Is Not Induced in the Pancreas of stat3$^{\Delta/\Delta}$ *Mice by Caerulein Treatment*

PAP1 was first discovered in the pancreas of rats with acute pancreatitis.[25] This protein was absent in control rats but appeared early after induction of pancreatitis and remained in an overexpressed state during inflammation. It is considered to be one of the acute-phase proteins. Serum levels of PAP1 have been reported to increase in patients with acute pancreatitis and to decrease steadily during recovery.[26] The expression of this secretory protein can be induced by several inflammatory cytokines and by itself through a JAK/STAT3-dependent pathway.[27] At least two functional STAT3-responsible elements have been reported in the promoter of gene encoding PAP1, so a regulatory link between PAP1 and STAT3 has been proposed.[28] We examined PAP1 expression during caerulein-induced pancreatitis. In *stat3*$^{flox/flox}$ mice, PAP1 was markedly induced by caerulein treatment in the injured pancreas at 3 hours after the last injection but not in the liver and the lung (Figure 4A). In sharp contrast, it was not observed in the pancreas of *stat3*$^{\Delta/\Delta}$ mice with caerulein treatment (Figure 4B). PAP1 was secreted in a STAT3-dependent manner from the injured pancreas during caerulein-induced pancreatitis.

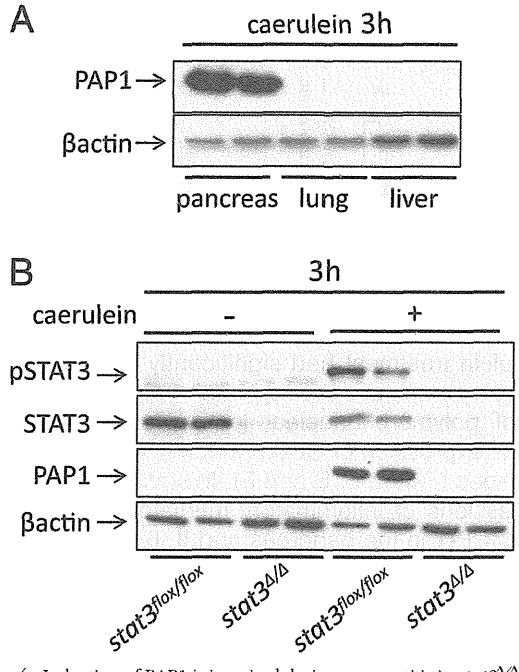

Figure 4. Induction of PAP1 is impaired during pancreatitis in *stat3*$^{\Delta/\Delta}$ mice. Acute pancreatitis was induced in *stat3*$^{\Delta/\Delta}$ and *stat3*$^{flox/flox}$ mice by eight hourly i.p. injections of caerulein for 2 consecutive days. The mice were sacrificed 3 hours after the last injection of caerulein. *stat3*$^{\Delta/\Delta}$ stands for *stat3*$^{flox/flox}$ *pdx1-Cre*. **A:** Expressions of PAP1 in caerulein-treated pancreas, lung, and liver of *stat3*$^{flox/flox}$ mice by Western blot analysis. β-Actin was included as a control. **B:** Expressions of STAT3, pSTAT3, and PAP1 in the pancreas were assessed by Western blot analysis. β-Actin was included as a control.

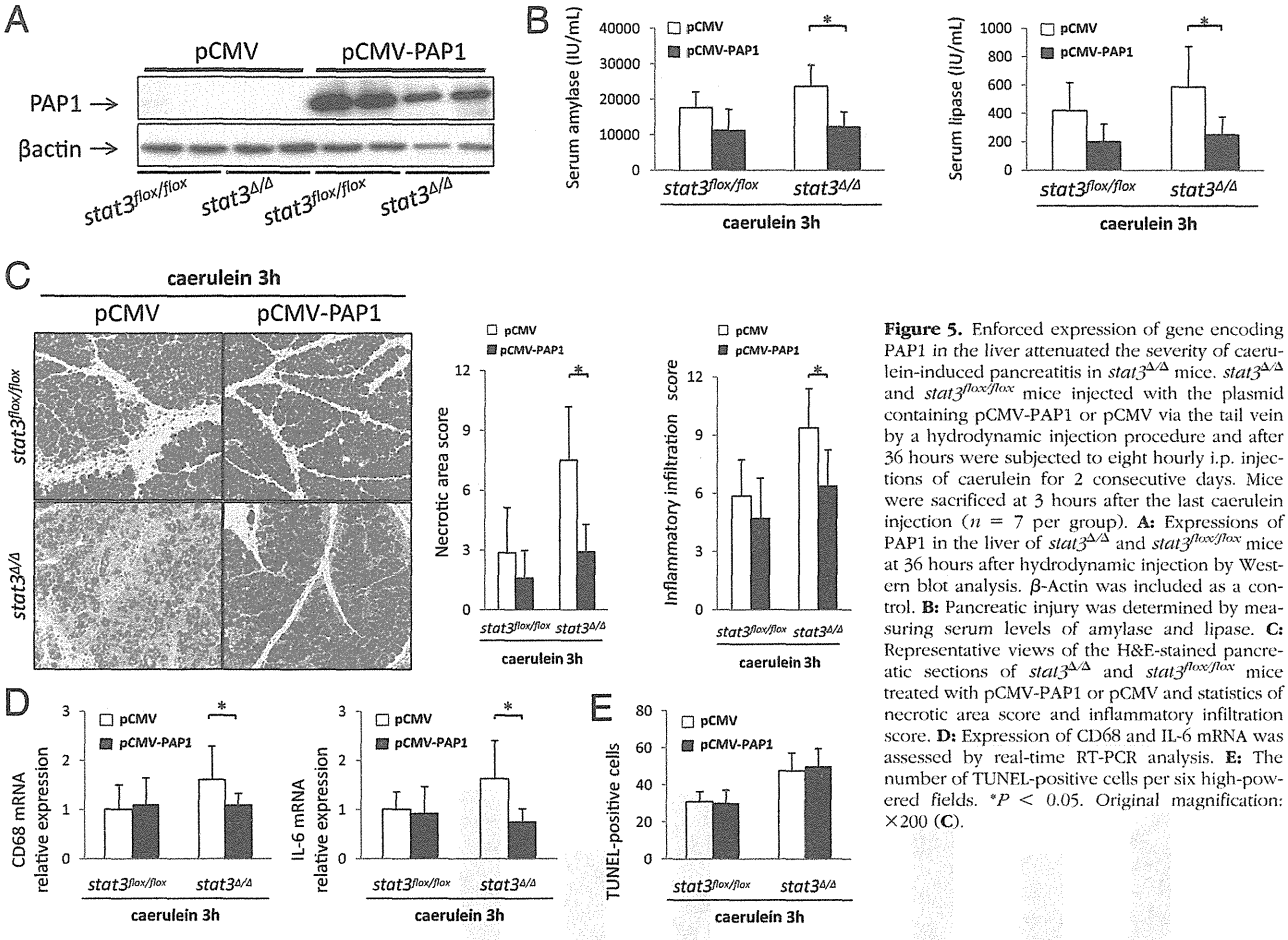

Figure 5. Enforced expression of gene encoding PAP1 in the liver attenuated the severity of caerulein-induced pancreatitis in *stat3*$^{\Delta/\Delta}$ mice. *stat3*$^{\Delta/\Delta}$ and *stat3*$^{flox/flox}$ mice injected with the plasmid containing pCMV-PAP1 or pCMV via the tail vein by a hydrodynamic injection procedure and after 36 hours were subjected to eight hourly i.p. injections of caerulein for 2 consecutive days. Mice were sacrificed at 3 hours after the last caerulein injection (n = 7 per group). **A:** Expressions of PAP1 in the liver of *stat3*$^{\Delta/\Delta}$ and *stat3*$^{flox/flox}$ mice at 36 hours after hydrodynamic injection by Western blot analysis. β-Actin was included as a control. **B:** Pancreatic injury was determined by measuring serum levels of amylase and lipase. **C:** Representative views of the H&E-stained pancreatic sections of *stat3*$^{\Delta/\Delta}$ and *stat3*$^{flox/flox}$ mice treated with pCMV-PAP1 or pCMV and statistics of necrotic area score and inflammatory infiltration score. **D:** Expression of CD68 and IL-6 mRNA was assessed by real-time RT-PCR analysis. **E:** The number of TUNEL-positive cells per six high-powered fields. $^*P < 0.05$. Original magnification: ×200 (**C**).

Enforced Expression of Gene Encoding PAP1 in the Liver Attenuates the Severity of Caerulein-Induced Pancreatitis and Promotes Pancreatic Recovery in stat3$^{\Delta/\Delta}$ *Mice*

To examine whether PAP1 deficiency in *stat3*$^{\Delta/\Delta}$ mice could be ascribed to exacerbation of caerulein-induced pancreatitis, enforced PAP1 expression was induced in the liver by a hydrodynamic injection procedure. Mice received pCMV-PAP1 or pCMV and after 36 hours were subjected to 2 days of caerulein treatment. PAP1 was clearly produced in the liver at 36 hours after hydrodynamic injection (Figure 5A). Both *stat3*$^{\Delta/\Delta}$ and *stat3*$^{flox/flox}$ mice treated with pCMV exhibited typical features of pancreatitis at 3 hours after the last caerulein injection (Figure 5, B and C). Of importance is the finding that the serum levels of amylase and lipase in *stat3*$^{\Delta/\Delta}$ mice injected with pCMV-PAP1 were significantly lower than those in *stat3*$^{\Delta/\Delta}$ mice injected with pCMV (Figure 5B). The extent of the necrotic area and the degree of inflammatory cell infiltration were significantly lower in *stat3*$^{\Delta/\Delta}$ mice treated with pCMV-PAP1 than those with pCMV injection (Figure 5C). Moreover, *stat3*$^{\Delta/\Delta}$ mice treated with pCMV-PAP1 had a marked decrease of the mRNA expressions of CD68 and IL-6 in the injured pancreas compared with those treated with pCMV (Figure 5D). In contrast, the number of TUNEL-positive cells did not differ in *stat3*$^{\Delta/\Delta}$ mice between the pCMV-PAP1 injection and pCMV injection groups (Figure 5E; see also Supplemental Figure S2A at *http://ajp.amjpathol.org*). We also examined the pancreatic recovery in *stat3*$^{\Delta/\Delta}$ mice pretreated with pCMV-PAP1 or pCMV at 3 days after the last caerulein injection. The PAP1-treated group had clear improvement of pancreas histologic findings (Figure 6A). The relative pancreatic weight of *stat3*$^{\Delta/\Delta}$ mice with PAP1 treatment significantly increased compared with those given the control treatment; it did not differ from that of *stat3*$^{flox/flox}$ mice (Figure 6B). In addition, the number of Ki-67 positive cells in *stat3*$^{\Delta/\Delta}$ mice with PAP1 treatment also significantly increased (Figure 6C). These results suggest that enforced PAP1 expression not only attenuated the severity of the necrotizing pancreatitis with infiltration of inflammatory cells but also promoted pancreatic recovery in *stat3*$^{\Delta/\Delta}$ mice with caerulein treatment.

Discussion

The STAT3 pathway is not essential for pancreatic organogenesis[29] but is required for the process of acinar-to-ductal metaplasia, which is observed not only in chronic inflammation but also in the pathogenesis of pancreatic ductal adenocarcinoma.[29] STAT3, which was found to be activated in human pancreatic ductal adenocarcinoma,[30] regulates a number of pathways impor-

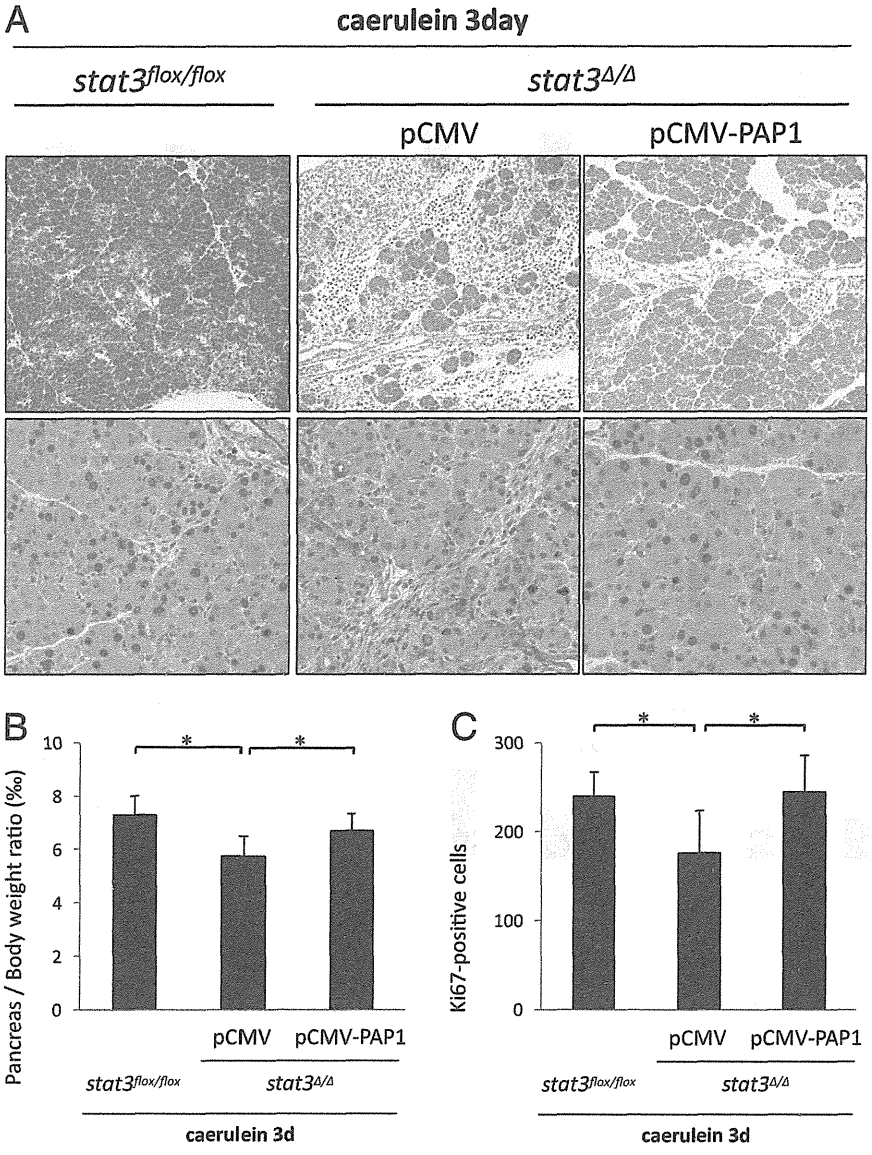

Figure 6. Enforced expression of gene encoding PAP1 in the liver promoted pancreas recovery in $stat3^{\Delta/\Delta}$ mice during caerulein-induced pancreatitis. At 36 hours before the first caerulein injection, $stat3^{\Delta/\Delta}$ mice were injected with pCMV-PAP1 or pCMV via the tail vein by a hydrodynamic injection procedure. Acute pancreatitis was induced in $stat3^{\Delta/\Delta}$ and $stat3^{flox/flox}$ mice by eight hourly i.p. injections of caerulein for 2 consecutive days. The mice were sacrificed at 3 days after the last injection of caerulein. **A:** Representative views of H&E staining (upper panels) and Ki-67 immunohistochemical staining (lower panels) of the pancreatic sections in $stat3^{flox/flox}$ and $stat3^{\Delta/\Delta}$ mice treated with pCMV-PAP1 or pCMV. **B:** Relative pancreatic weight in $stat3^{flox/flox}$ and $stat3^{\Delta/\Delta}$ mice treated with pCMV-PAP1 or pCMV ($n = 3$ per $stat3^{flox/flox}$ group, $n = 6$ per the other groups). **C:** Statistics of Ki-67 positive cells per four high-powered fields ($n = 3$ per $stat3^{flox/flox}$ group, $n = 6$ per the other groups). $^*P < 0.05$. Original magnification: ×200 (**C**); ×400 (**D**).

tant in tumorigenesis, including cell cycle progression, apoptosis, tumor angiogenesis, invasion, and metastasis.[30–32] Although previous work has suggested the importance of pancreatic STAT3 in carcinogenesis, its role in acute inflammation had not been formally examined. In the present study, we demonstrated that genetic ablation of STAT3 in the pancreas exacerbated the course of caerulein-induced acute pancreatitis. $stat3^{\Delta/\Delta}$ mice had a clear increase in the number of pancreatic inflammatory cells and the levels of pancreatic and circulating inflammatory cytokines, leading to massive pancreatic necrotic change. Our data demonstrate that pancreatic STAT3 has a protective effect against necrotizing pancreatitis with numerous inflammatory infiltrations *in vivo*. Moreover, $stat3^{\Delta/\Delta}$ mice with caerulein treatment had a marked decrease of PAP1 compared with $stat3^{flox/flox}$ mice. PAP1 is a secretory protein, and enforced expression of gene encoding PAP1 in the liver of $stat3^{\Delta/\Delta}$ mice significantly improved pancreatic necrosis, inflammatory infiltration, and pancreatic recovery during acute pancreatitis. This is the first report, to our knowledge, to demonstrate that the STAT3/PAP1 pathway plays an important role in protection against caerulein-induced pancreatitis.

Research has shown that PAP1 has anti-inflammatory and antiapoptotic activities[27,33,34] and may be involved in cellular proliferation.[35,36] PAP1 was discovered in the pancreatic juice of rats after induction of acute pancreatitis, but expression of this secretory protein is not restricted to pancreatic tissue. PAP1 has been observed in several tissues during injuries, including the intestine of inflammatory bowel diseases[37] and sensory neurons after peripheral injury.[38] In the exocrine pancreas, PAP1 is only expressed in response to many pancreatic injuries, such as pancreatitis, hypoxia, and lipopolysaccharide injection, as well as in the transplanted tissue.[39–42] The absence of PAP1 from the healthy tissues and its strong induction observed during the early phase of the disease suggest that PAP1 could be an acute-phase protein induced on tissue injury. In the present study, although caerulein treatment induced strong expression of PAP1 in

the pancreas, but not in other organs, PAP1 was not induced in *stat3*$^{\Delta/\Delta}$ mice. This finding indicates that PAP1 is expressed in a STAT3-dependent manner from the injured pancreas during acute pancreatitis.

Anti-inflammatory activity of PAP1 in the pancreas has been reported in *in vitro* and *in vivo* studies. In the AR42J pancreatic acinar cell line, purified PAP1 protein inhibited NF-κB activation and production of IL-6 and TNF-α in response to TN-Fα.[43] A recent study found that traditional *PAP1* knockout mice, on caerulein treatment, had more inflammatory cell infiltration and proinflammatory cytokine production in the pancreas than WT mice and that administration of recombinant PAP1 repressed the inflammatory responses.[44] Another group reported that conditional *rela/p65* knockout mice had marked decrease of PAP1 production and exacerbated pancreatic necrosis and inflammatory cell infiltration during caerulein-induced pancreatitis. This study also demonstrated that knockdown of gene encoding PAP1 in WT mice led to exacerbated necrotizing pancreatitis with inflammatory cell infiltration and that lentiviral gene transfer of *PAP1* cDNA reduced the extent of necrosis and inflammatory responses in the pancreas of *rela/p65* knockout mice.[45] In the present study, *stat3*$^{\Delta/\Delta}$ mice had severe inflammatory responses and necrosis during caerulein-induced pancreatitis, which were clearly suppressed by PAP1 treatment. This finding is in agreement with the well-recognized anti-inflammatory role of PAP1 and suggests a close link between inflammation and necrosis during pancreatitis. Traditional *PAP1* knockout mice with caerulein treatment had severer inflammation but less severe necrosis in the pancreas.[44] These results were inconsistent with ours and the data from another group.[45] Although the reason for this inconsistency is not clear, it may involve the difference in protocols of caerulein treatment, which could affect the severity of the acute pancreatitis.

Recent studies have demonstrated that overexpression of PAP1 prevented apoptosis induced by oxidative stress or TNF-α stimulation in AR42J cells.[46,47] In traditional *PAP1* knockout mice, the pancreas was sensitive to apoptosis during caerulein-induced pancreatitis, and PAP1 treatment reduced pancreatic apoptosis induced by caerulein injection.[44] In the present study, *stat3*$^{\Delta/\Delta}$ mice showed increased apoptosis and necrosis during acute pancreatitis. STAT3 is known to regulate several gene expressions of antiapoptotic proteins, such as Bcl-xL and Mcl-1.[48,49] Caerulein treatment induced up-regulation of Bcl-xL in the pancreas of *stat3*$^{flox/flox}$ mice, whereas the up-regulation of this protein was impaired in *stat3*$^{\Delta/\Delta}$ mice (see Supplemental Figure S2B at *http://ajp.amjpathol.org*). This result indicated that Bcl-xL is up-regulated during pancreatitis, depending on STAT3, and suggested that impaired Bcl-xL induction may be involved in the susceptibility to apoptosis in *stat3*$^{\Delta/\Delta}$ pancreas. Interestingly, PAP1 treatment in *stat3*$^{\Delta/\Delta}$ mice significantly reduced the extent of necrosis but did not affect apoptosis. In agreement with this, Western blotting analysis revealed that impaired expression of Bcl-xL in *stat3*$^{\Delta/\Delta}$ mice was still observed even with PAP1 treatment (see Supplemental Figure S2B at *http://ajp.amjpathol.org*). Although it remains obscure why PAP1 treatment had no effect on apoptosis in our model, the antiapoptotic effect of PAP1 might be dependent on pancreatic STAT3 signaling during pancreatitis.

Pancreatic recovery was delayed in *stat3*$^{\Delta/\Delta}$ mice during acute pancreatitis, and PAP1 treatment promoted its recovery. Although STAT3 activation has been linked to the regeneration process,[14,32] PAP1 has been also reported to be associated with tissue regeneration and cellular proliferation in the liver and the intestine.[35,36] Our data demonstrated that deficiency of STAT3 caused severe pancreatic injury early in pancreatitis. This drastic damage of pancreas may lead to the delayed recovery in *stat3*$^{\Delta/\Delta}$ mice during caerulein-induced pancreatitis, although the involvement of pancreatic STAT3 or PAP1 in the regeneration phase of the injured pancreas remains obscure in our model. The contribution of pancreatic STAT3 or PAP1 in regeneration needs to be elucidated in further studies using other models of pancreatic regeneration, such as partial pancreatectomy.

In conclusion, our data demonstrate that pancreatic STAT3 is indispensable for inducing PAP1 production in the injured pancreas during acute pancreatitis and that activation of pancreatic STAT3 leads to protective effects against pancreatic injury and inflammation via PAP1 production.

References

1. Raraty MG, Murphy JA, Mcloughlin E, Smith D, Criddle D, Sutton R: Mechanisms of acinar cell injury in acute pancreatitis. Scand J Surg 2005, 94:89–96
2. Saluja AK, Donovan EA, Yamanaka K, Yamaguchi Y, Hofbauer B, Steer ML: Cerulein-induced in vitro activation of trypsinogen in rat pancreatic acini is mediated by cathepsin B. Gastroenterology 1997, 113:304–310
3. Norman J: The role of cytokines in the pathogenesis of acute pancreatitis. Am J Surg 1998, 175:76–83
4. Bhatia M, Brady M, Shokuhi S, Christmas S, Neoptolemos JP, Slavin J: Inflammatory mediators in acute pancreatitis. J Pathol 2000, 190: 117–125
5. Bhatia M, Wong FL, Cao Y, Lau HY, Huang J, Puneet P, Chevali L: Pathophysiology of acute pancreatitis. Pancreatology 2005, 5:132–144
6. Pooran N, Indaram A, Singh P, Bank S: Cytokines (IL-6. IL-8, TNF): early and reliable predictors of severe acute pancreatitis. J Clin Gastroenterol 2003, 37:263–266
7. Mayer J, Rau B, Gansauge F, Beger HG: Inflammatory mediators in human acute pancreatitis: clinical and pathophysiological implications. Gut 2000, 47:546–552
8. Dugernier TL, Laterre PF, Wittebole X, Roeseler J, Latinne D, Reynaert MS, Pugin J: Compartmentalization of the inflammatory response during acute pancreatitis: correlation with local and systemic complications. Am J Respir Crit Care Med 2003, 168:148–157
9. O'Shea JJ, Gadina M, Schreiber RD: Cytokine signaling in 2002: new surprises in the Jak/Stat pathway. Cell 2002, 109(Suppl):S121–S131
10. Akira S, Nishio Y, Inoue M, Wang XJ, Wei S, Matsusaka T, Yoshida K, Sudo T, Naruto M, Kishimoto T: Molecular cloning of APRF, a novel IFN-stimulated gene factor 3 p91-related transcription factor involved in the gp130-mediated signaling pathway. Cell 1994, 77:63–71
11. Zhong Z, Wen Z, Darnell JE: Stat3: a STAT family member activated by tyrosine phosphorylation in response to epidermal growth factor and interleukin-6. Science 1994, 264:95–98
12. Kobierski LA, Srivastava S, Borsook D: Systemic lipopolysaccharide and interleukin-1beta activate the interleukin 6: sTAT intracellular

signaling pathway in neurons of mouse trigeminal ganglion. Neurosci Lett 2000, 281:61–64
13. Obana M, Maeda M, Takeda K, Hayama A, Mohri T, Yamashita T, Nakaoka Y, Komuro I, Matsumiya G, Azuma J, Fujio Y: Therapeutic activation of signal transducer and activator of transcription 3 by interleukin-11 ameliorates cardiac fibrosis after myocardial infarction. Circulation 2010, 121:684–691
14. Li W, Liang X, Kellendonk C, Poli V, Taub R: STAT3 contributes to the mitogenic response of hepatocytes during liver regeneration. J Biol Chem 2002, 277:28411–28417
15. Sakamori R, Takehara T, Ohnishi C, Tatsumi T, Ohkawa K, Takeda K, Akira S, Hayashi N: Signal transducer and activator of transcription 3 signaling within hepatocytes attenuates systemic inflammatory response and lethality in septic mice. Hepatology 2007, 46:1564–1573
16. Robinson K, Vona-Davis L, Riggs D, Jackson B, McFadden D: Peptide YY attenuates STAT1 and STAT3 activation induced by TNF-alpha in acinar cell line AR42J. J Am Coll Surg 2006, 202:788–796
17. Vona-Davis LC, Frankenberry KA, Waheed U, Peterson E, McFadden DW: Expression of STAT3 and SOCS3 in pancreatic acinar cells. J Surg Res 2005, 127:14–120
18. Yubero S, Ramudo L, Manso MA, De Dios I: The role of redox status on chemokine expression in acute pancreatitis. Biochim Biophys Acta 2009, 1792:148–154
19. Takeda K, Noguchi K, Shi W, Tanaka T, Matsumoto M, Yoshida N, Kishimoto T, Akira S: Targeted disruption of the mouse Stat3 gene leads to early embryonic lethality. Proc Natl Acad Sci U S A 1997, 94:3801–3804
20. Takeda K, Kaisho T, Yoshida N, Takeda J, Kishimoto T, Akira S: Stat3 activation is responsible for IL-6-dependent T cell proliferation through preventing apoptosis: generation and characterization of T cell-specific Stat3-deficient mice. J Immunol 1998, 161:4652–4660
21. Shigekawa M, Takehara T, Kodama T, Hikita H, Shimizu S, Li W, Miyagi T, Hosui A, Tatsumi T, Ishida H, Kanto T, Hiramatsu N, Hayashi N: Involvement of STAT3-regulated hepatic soluble factors in attenuation of stellate cell activity and liver fibrogenesis in mice. Biochem Biophys Res Commun 2011, 406:614–620
22. Uemura A, Takehara T, Miyagi T, Suzuki T, Tatsumi T, Ohkawa K, Kanto T, Hiramatsu N, Hayashi N: Natural killer cell is a major producer of interferon gamma that is critical for the IL-12-induced anti-tumor effect in mice. Cancer Immunol Immunother 2010, 59:453–463
23. Chen C, Fang R, Davis C, Maravelias C, Sibley E: Pdx1 inactivation restricted to the intestinal epithelium in mice alters duodenal gene expression in enterocytes and enteroendocrine cells. Am J Physiol Gastrointest Liver Physiol 2009, 297:G1126–G1137
24. Jensen JN, Cameron E, Garay MV, Starkey TW, Gianani R, Jensen J: Recapitulation of elements of embryonic development in adult mouse pancreatic regeneration. Gastroenterology 2005, 128:728–741
25. Keim V, Rohr G, Stöckert HG, Haberich FJ: An additional secretory protein in the rat pancreas. Digestion 1984, 29:242–249
26. Iovanna JL, Keim V, Nordback I, Montalto G, Camarena J, Letoublon C, Lévy P, Berthézène P, Dagorn JC, Multicentric Study Group on Acute Pancreatitis: Serum levels of pancreatitis-associated protein as indicators of the course of acute pancreatitis. Gastroenterology 1994, 106:728–734
27. Folch-Puy E, Granell S, Dagorn JC, Iovanna JL, Closa D: Pancreatitis-associated protein I suppresses NF-kappa B activation through a JAK/STAT-mediated mechanism in epithelial cells. J Immunol 2006, 176:3774–3779
28. Dusetti NJ, Ortiz EM, Mallo GV, Dagorn JC, Iovanna JL: Pancreatitis-associated protein I (PAP I), an acute phase protein induced by cytokines. Identification of two functional interleukin-6 response elements in the rat PAP I promoter region J Biol Chem 1995, 270:22417–22421
29. Miyatsuka T, Kaneto H, Shiraiwa T, Matsuoka TA, Yamamoto K, Kato K, Nakamura Y, Akira S, Takeda K, Kajimoto Y, Yamasaki Y, Sandgren EP, Kawaguchi Y, Wright CV, Fujitani Y: Persistent expression of PDX-1 in the pancreas causes acinar-to-ductal metaplasia through Stat3 activation. Genes Dev 2006, 20:1435–1440
30. Scholz A, Heinze S, Detjen KM, Peters M, Welzel M, Hauff P, Schirner M, Wiedenmann B, Rosewicz S: Activated signal transducer and activator of transcription 3 (STAT3) supports the malignant phenotype of human pancreatic cancer. Gastroenterology 2003, 125:891–905
31. Greten FR, Weber CK, Greten TF, Schneider G, Wagner M, Adler G, Schmid RM: Stat3 and NF-kappaB activation prevents apoptosis in pancreatic carcinogenesis. Gastroenterology 2002, 123:2052–2063
32. Aggarwal BB, Kunnumakkara AB, Harikumar KB, Gupta SR, Tharakan ST, Koca C, Dey S, Sung B: Signal transducer and activator of transcription-3, inflammation, and cancer: how intimate is the relationship? Ann N Y Acad Sci 2009, 1171:59–76
33. Moniaux N, Song H, Darnaud M, Garbin K, Gigou M, Mitchell C, Samuel D, Jamot L, Amouyal P, Amouyal G, Bréchot C, Faivre J: Human hepatocarcinoma-intestine-pancreas/pancreatitis-associated protein cures fas-induced acute liver failure in mice by attenuating free-radical damage in injured livers. Hepatology 2011, 53:618–627
34. Gironella M, Iovanna JL, Sans M, Gil F, Peñalva M, Closa D, Miquel R, Piqué JM, Panés J: Anti-inflammatory effects of pancreatitis associated protein in inflammatory bowel disease. Gut 2005, 54:1244–1253
35. Moucadel V, Soubeyran P, Vasseur S, Dusetti NJ, Dagorn JC, Iovanna JL: Cdx1 promotes cellular growth of epithelial intestinal cells through induction of the secretory protein PAP I. Eur J Cell Biol 2001, 80:156–163
36. Simon MT, Pauloin A, Normand G, Lieu HT, Mouly H, Pivert G, Carnot F, Tralhao JG, Brechot C, Christa L: HIP/PAP stimulates liver regeneration after partial hepatectomy and combines mitogenic and anti-apoptotic functions through the PKA signaling pathway. FASEB J 2003, 17:1441–1450
37. Dieckgraefe BK, Stenson WF, Korzenik JR, Swanson PE, Harrington CA: Analysis of mucosal gene expression in inflammatory bowel disease by parallel oligonucleotide arrays. Physiol Genomics 2000, 4:1–11
38. Averill S, Davis DR, Shortland PJ, Priestley JV, Hunt SP: Dynamic pattern of reg-2 expression in rat sensory neurons after peripheral nerve injury. J Neurosci 2002, 22:7493–7501
39. Orelle B, Keim V, Masciotra L, Dagorn JC, Iovanna JL: Human pancreatitis-associated protein. Messenger RNA cloning and expression in pancreatic diseases. J Clin Invest 1992, 90:2284–2291
40. McKie AT, Simpson RJ, Ghosh S, Peters TJ, Farzaneh F: Regulation of pancreatitis-associated protein (HIP/PAP) mRNA levels in mouse pancreas and small intestine. Clin Sci (Lond) 1996, 91:213–218
41. Vaccaro MI, Calvo EL, Suburo AM, Sordelli DO, Lanosa G, Iovanna JL: Lipopolysaccharide directly affects pancreatic acinar cells: implications on acute pancreatitis pathophysiology. Dig Dis Sci 2000, 45:915–926
42. van der Pijl JW, Boonstra JG, Barthellemy S, Smets YF, Hermans J, Bruijn JA, de Fijter JW, Daha MR, Dagorn JC: Pancreatitis-associated protein: a putative marker for pancreas graft rejection. Transplantation 1997, 63:995–1003
43. Vasseur S, Folch-Puy E, Hlouschek V, Garcia S, Fiedler F, Lerch MM, Dagorn JC, Closa D, Iovanna JL: p8 improves pancreatic response to acute pancreatitis by enhancing the expression of the anti-inflammatory protein pancreatitis-associated protein I. J Biol Chem 2004, 279:7199–7207
44. Gironella M, Folch-Puy E, LeGoffic A, Garcia S, Christa L, Smith A, Tebar L, Hunt SP, Bayne R, Smith AJ, Dagorn JC, Closa D, Iovanna JL: Experimental acute pancreatitis in PAP/HIP knock-out mice. Gut 2007, 56:1091–1097
45. Algül H, Treiber M, Lesina M, Nakhai H, Saur D, Geisler F, Pfeifer A, Paxian S, Schmid RM: Pancreas-specific RelA/p65 truncation increases susceptibility of acini to inflammation-associated cell death following cerulein pancreatitis. J Clin Invest 2007, 117:1490–1501
46. Ortiz EM, Dusetti NJ, Vasseur S, Malka D, Bödeker H, Dagorn JC, Iovanna JL: The pancreatitis-associated protein is induced by free radicals in AR4-2J cells and confers cell resistance to apoptosis. Gastroenterology 1998, 114:808–816
47. Malka D, Vasseur S, Bödeker H, Ortiz EM, Dusetti NJ, Verrando P, Dagorn JC, Iovanna JL: Tumor necrosis factor alpha triggers antiapoptotic mechanisms in rat pancreatic cells through pancreatitis-associated protein I activation. Gastroenterology 2000, 119:816–828
48. Yu H, Pardoll D, Jove R: STATs in cancer inflammation and immunity: a leading role for STAT3. Nat Rev Cancer 2009, 9:798–809
49. Epling-Burnette PK, Liu JH, Catlett-Falcone R, Turkson J, Oshiro M, Kothapalli R, Li Y, Wang JM, Yang-Yen HF, Karras J, Jove R, Loughran TP: Inhibition of STAT3 signaling leads to apoptosis of leukemic large granular lymphocytes and decreased Mcl-1 expression. J Clin Invest 2001, 107:351–362

Cancer Immunol Immunother (2012) 61:1425–1432
DOI 10.1007/s00262-012-1208-6

ORIGINAL ARTICLE

Interleukin-1β enhances the production of soluble MICA in human hepatocellular carcinoma

Keisuke Kohga · Tomohide Tatsumi · Hinako Tsunematsu · Satoshi Aono · Satoshi Shimizu · Takahiro Kodama · Hayato Hikita · Masashi Yamamoto · Tsugiko Oze · Hiroshi Aketa · Atsushi Hosui · Takuya Miyagi · Hisashi Ishida · Naoki Hiramatsu · Tatsuya Kanto · Norio Hayashi · Tetsuo Takehara

Received: 15 July 2011 / Accepted: 17 January 2012 / Published online: 1 February 2012

Abstract The production of soluble major histocompatibility complex class I–related chain A (MICA) is thought to antagonize NKG2D-mediated immunosurveillance. Interleukin-1β (IL-1β) is elevated in patients with chronic hepatitis C (CH), and this might contribute to the escape of hepatocellular carcinoma (HCC) cells from innate immunity. In this study, we investigated the immunoregulatory role of IL-1β in the production of soluble MICA of HCC cells. First, we investigated the correlation between the serum IL-1β levels and soluble MICA in CH patients. Serum IL-1β levels were associated with soluble MICA levels in CH patients. The serum IL-1β levels of CH patients with the HCC occurrence were significantly higher than those of CH patients without HCC. We next examined the MICA production of IL-1β-treated HCC cells. Addition of IL-1β resulted in significant increase in the production of soluble MICA in HepG2 and PLC/PRF/5 cells, human HCC cells. But soluble MICA was not detected in both non-treated and IL-1β-treated normal hepatocytes. Addition of IL-1β did not increase the expressions of membrane-bound MICA on HCC cells. These were observed similarly in various cancer cells including a gastric cancer (MKN1), two colon cancers (HCT116 and HT29) and a cervical cancer (HeLa). Addition of IL-1β also increased the expression of a disintegrin and metalloproteinase (ADAM)9 in HCC cells, and the knockdown of ADAM9 in IL-1β-treated HCC cells resulted in the decrease in the production of soluble MICA of HCC cells. These findings indicate that IL-1β might enhance the production of soluble MICA by activating ADAM9 in human HCC.

Keywords IL-1β · Hepatocellular carcinoma · Soluble MICA · ADAM9

Abbreviations

IL	Interleukin
HCC	Hepatocellular carcinoma
MICA	Major histocompatibility complex class I–related chain A
ADAM9	A disintegrin and metalloproteinase 9

Introduction

Interleukin-1β (IL-1β) is a proinflammatory cytokine with multiple biological effects [1]. Serum levels of IL-1β are elevated in patients infected with hepatitis C virus (HCV), suggesting the role of IL-1β in the inflammation of liver [2–4]. Several polymorphisms of the IL-1 gene have been reported to affect IL-1β production [5, 6]. A number of clinical studies suggested that polymorphisms of IL-1β gene are associated with diverse disease including cancer [5, 7]. IL-1β gene polymorphisms have also been reported to be associated with HCC in HCV- or HBV-infected patients [8–10]. While genetic studies have suggested an important role for IL-1β in cancer, direct evidence that IL-1β contributes to the pathogenesis of cancer has been lacking. Recently,

Keisuke Kohga and Tomohide Tatsumi have equally contributed to this work and share the first authorship.

K. Kohga · T. Tatsumi (✉) · H. Tsunematsu · S. Aono · S. Shimizu · T. Kodama · H. Hikita · M. Yamamoto · T. Oze · H. Aketa · A. Hosui · T. Miyagi · H. Ishida · N. Hiramatsu · T. Kanto · N. Hayashi · T. Takehara
Department of Gastroenterology and Hepatology, Osaka University Graduate School of Medicine, 2-2 Yamadaoka, Suita, Osaka 565-0871, Japan
e-mail: tatsumit@gh.med.osaka-u.ac.jp

N. Hayashi
Kansai-Rosai Hospital, Amagasaki, Hyogo 660-8511, Japan

Tu et al. [11] reported that stomach-specific expression of IL-1β in transgenic mice leads to spontaneous gastric inflammation and cancer that correlates with myeloid-derived suppressor cells to the stomach. However, no studies have been published on the direct effect of IL-1β on the HCC cells in patients infected with HCV.

MHC class I–related chain A (MICA), a ligand for NKG2D, is rarely expressed on normal cells, but frequently on tumor cells [12, 13]. The engagement of MICA and NKG2D strongly activates NK cells enhancing their cytolytic activity and cytokine production [14]. Thus, the MICA-NKG2D pathway is an important mechanism by which the host immune system recognizes and kills transformed cells [15]. In addition to those membrane-bound forms, MICA molecules are cleaved proteolytically from tumor cells and appear as soluble forms in the sera of patients with malignancy including HCC [16–18]. The release of soluble MICA/B from tumor cells is thought to antagonize NKG2D-mediated immunosurveillance. We previously demonstrated that a disintegrin and metalloproteinase (ADAM)9 protease plays essential roles in the shedding of MICA molecules on HCC cells [19]. However, the mechanism of regulating the production of soluble MICA in HCC cells remains to be elucidated.

In this study, we investigated the immunoregulatory role of IL-1β in the production of soluble MICA from HCC cells. Of importance is the discovery that the serum IL-1β levels in chronic hepatitis patients with the HCC occurrence were significantly higher than those without HCC occurrence and that IL-1β enhances the production of soluble MICA via activating ADAM9 in human HCC cells. The present study sheds light on previously unrecognized immunological effects of IL-1β on HCC cells.

Materials and methods

HCC cell lines and normal hepatocyte cultures

HepG2 and PLC/PRF/5, human HCC cell lines, were purchased from American Type Culture Collection (Rockville, MD) and were cultured with Dulbecco's Modified Eagle's Medium supplemented with 10% fetal bovine serum (GIBCO/Life Technologies, Grand Island, NY) in a humidified incubator at 5% CO_2 and 37°C. 2×10^5 HepG2 and PLC/PRF/5 cells or normal hepatocytes (ScienCell Research Laboratories, Carlsbad, CA) were cultured in 6-well tissue culture plates for 48 h in the presence or absence of human interleukin-1β (IL-1β) (50 ng/ml, PeproTech EC, London, UK), and the HCC cells were harvested and subjected to evaluating the expression of membrane-bound MICA and ADAM9 and the production of soluble MICA.

Flow cytometry

For the detection of membrane-bound MICA, HCC cells were incubated with anti-MICA-specific Ab (Santa Cruz Biotechnology, Santa Cruz, CA) and stained with Goat $F(ab')2$ fragment anti-mouse IgG($H + L$) − PE (Beckman Coulter, Fullerton, CA) as a secondary reagent. Flow cytometric analysis was performed using a FACScan flow cytometer (Becton–Dickinson, San Jose, CA).

Western blotting

The total cellular protein was electrophoretically separated by sodium dodecyl sulfate-12% polyacrylamide gels and transferred onto PVDF membrane. The membrane was blocked in Tris-buffered saline–Tween containing 5% skim milk for 1 h and then probed with anti-ADAM9 mAb (R&D Systems, Minneapolis, MN) at 4°C overnight. Horseradish peroxidase-conjugated anti-rabbit Ab and SuperSignal West Pico System (Pierce, Rockford, IL) were used for the detection of blots.

Real-time reverse transcription (RT) PCR

Total RNA was isolated using RNeasy Mini Kit (Qiagen K.K., Tokyo, Japan) and was reverse transcribed using High Capacity RNA-to-cDNA Master Mix (Applied Biosystems, Foster city, CA). The mRNA levels were evaluated using ABI PRISM 7900 Sequence Detection System (Applied Biosystems). Ready-to-use assays (Applied Biosystems) were used for the quantification of ADAM9 (Hs00177638_m1), MICA (Hs00792195_m1) and β-actin (Hs99999903_m1) mRNAs according to the manufacturer's instructions. β-Actin mRNA from each sample was quantified as an endogenous control of internal RNA.

RNA silencing

The small interfering RNA (siRNA) method was used to knockdown ADAM9 as previously described [19]. At 24-h post-transfection, the cells were analyzed for specific depletion of the protein of ADAM9 by western blotting. The following siRNA were used: ADAM9, 5′-UGUCCAAAC ACAUUAAUCCCGCCUG-3′; an irrelevant siRNA as a control, 5′-UGUCGCACAAACACUUAACUCCCUG-3′.

ELISA

The sera from chronic hepatitis C patients ($N = 24$) with or without the occurrence of HCC were subjected to analysis of IL-1β and soluble MICA. Informed consent, under an Institutional Review Board–approved protocol, was obtained from all patients before sample acquisition.

The sera and the supernatants of cultured HCC cells were harvested, and the levels of IL-1β and soluble MICA were determined by human IL-1β ELISA set II (BD Biosciences, San Diego, CA) and DuoSet MICA eELISA kit (R&D Systems, Minneapolis, MN) in accordance with the manufacturer's instructions, respectively.

NK cell analysis

NK cells were isolated from human peripheral blood mononuclear cells by magnetic cell sorting using CD56 MicroBeads (Miltenyi Biotech, Auburn, CA) as previously described [19]. HepG2 and PLC/PRF/5 cells were treated with IL-1β (50 ng/ml) for 48 h. The cytolytic ability of NK cells against IL-1β-treated or non-treated HepG2 and PLC/PRF/5 cells was assessed by 4-hr ^{51}Cr-releasing assay as previously described [19].

Statistics

All values were expressed as the mean and SD. The statistical significance of differences between the groups was determined by applying Student's t test or two-sample t test with Welch correction after each group had been tested with equal variance and Fisher's exact probability test. We defined statistical significance as $p < 0.05$.

Results

Serum IL-1β levels were associated with soluble MICA in chronic liver disease patients

We first examined the IL-1β levels and soluble MICA levels of twenty-four chronic hepatitis C (CH) patients. Serum IL-1β levels in CH patients correlated with soluble MICA levels (Fig. 1a). We next examined the serum IL-1β levels of CH patients with or without the occurrence of HCC. We examined serum IL-1β levels of these 24 CH patients before HCC occurrence and followed these patients for 5 years. CH patients could be divided into two groups according to the occurrence of HCC (Table 1). As shown in Fig. 1b, the serum IL-1β levels of patients with the occurrence of HCC ($n = 11$) were significantly higher than those of patients without the occurrence of HCC ($n = 13$). These results suggested that the elevation of serum IL-1β levels might be associated with the occurrence of HCC in CH patients.

IL-1β increases the production of soluble MICA from HCC cells, but not from normal hepatocytes

We examined whether IL-1β treatment could induce MICA expressions on HCC cells (PLC/PRF/5 cells and HepG2 cells). Both PLC/PRF/5 cells and HepG2 cells were cultured for 48 h with IL-1β (50 ng/ml) and then subjected to analysis of the expression of membrane-bound MICA and mRNA of MICA. The expression of membrane-bound MICA of IL-1β-treated HCC cells was similar to that of non-treated HCC cells (Fig. 2a). IL-1β treatment induced significant increase of mRNA of MICA in PLC/PRF/5 cells, but this did not in HepG2 cells (Fig. 2b). We next examined the production of soluble MICA in the supernatants of the IL-1β-treated HCC cells. IL-1β treatment

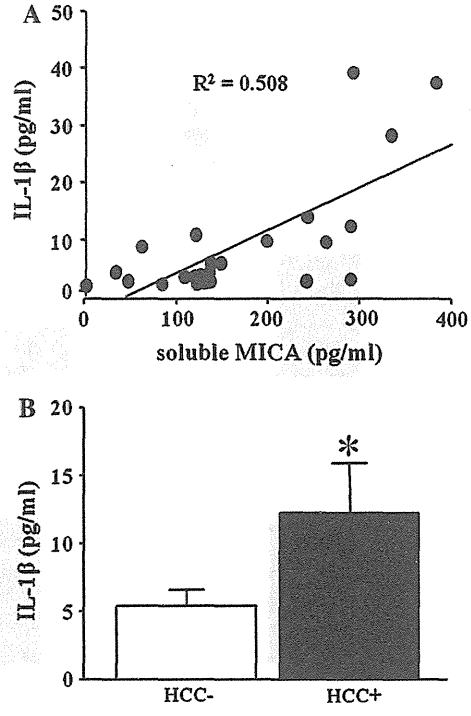

Fig. 1 The correlation between serum IL-1β and soluble MICA in patients with chronic liver disease and serum IL-1β levels in chronic liver disease patients with or without the HCC occurrence. **a** Correlation between serum IL-1β levels and soluble MICA levels in patients with chronic liver disease ($N = 24$). The serum IL-1β and soluble MICA were evaluated by specific ELISA, respectively. **b** Serum IL-1β levels in chronic hepatitis patients with HCC occurrence (HCC+, $N = 11$) or without HCC occurrence (HCC−, $N = 13$) were evaluated by specific ELISA. All patients were HCV-RNA-positive. *$p < 0.05$

Table 1 Clinical backgrounds

	HCC(+)	HCC(−)
Number	11	13
Age	61 ± 6	61 ± 8
Gender (M/F)	8/3	11/2
Platelet ($\times 10^4/\mu l$)	15 ± 5	14 ± 3
ALT (IU/l)	122 ± 109	89 ± 44

HCC(+) chronic hepatitis C patients with the occurrence of HCC, *HCC*(−) chronic hepatitis C patients without the occurrence of HCC, *M* male, *F* female, *ALT* alanine aminotransferase

resulted in the significant increase in the production of soluble MICA in both PLC/PRF/5 and HepG2 cells (Fig. 2c). These results demonstrated that the addition of IL-1β did not change the expression of membrane-bound MICA but resulted in significant increase in the production of soluble MICA in HCC cells. We also examined the effect of IL-1β on normal hepatocytes. As shown in Fig. 2d, normal hepatocytes did not produce soluble MICA and the addition of IL-1β did not result in its production.

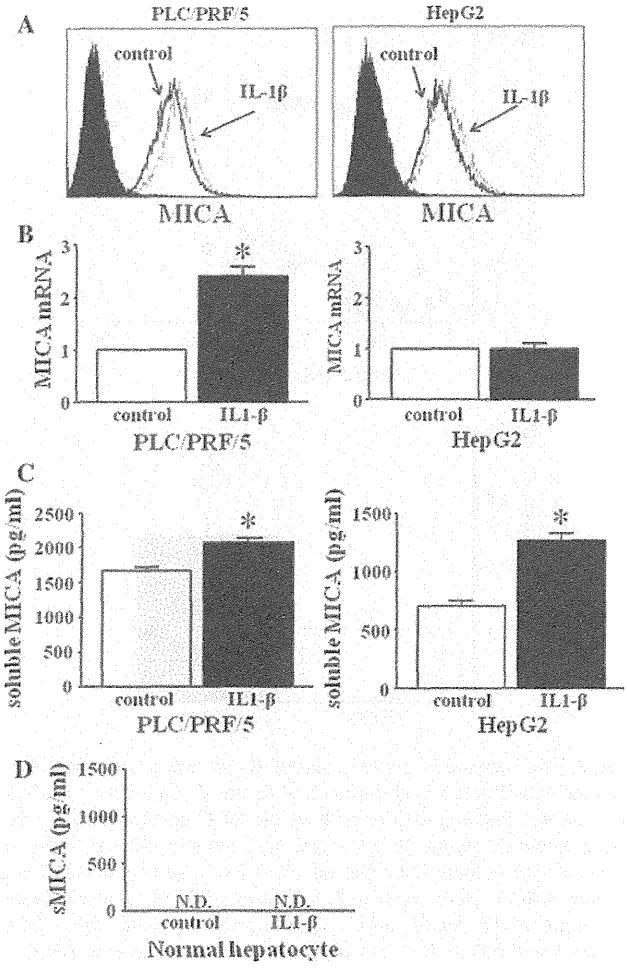

Fig. 2 Expression of membrane-bound MICA and the production of soluble MICA in IL-1β-treated HCC cells and normal hepatocytes. Both PLC/PRF/5 cells and HepG2 cells were treated in the presence or absence of IL-1β (50 ng/ml) for 48 h. The expression of membrane-bound MICA (**a**) and mRNA expression of MICA (**b**) in IL-1β-treated or non-treated HCC cells were evaluated by flow cytometry or real-time RT-PCR, respectively. *Black line histograms*, MICA staining of non-treated cells; *dotted line histograms*, MICA staining of IL-1β-treated cells; *shaded/black histograms*, control IgG isotype Ab staining. Similar results were obtained from two independent experiments. $*p < 0.05$. **c** We examined the production of soluble MICA on IL-1β-treated or non-treated HCC cells by specific ELISA. $*p < 0.05$. **d** Normal hepatocytes were treated in the presence or absence of IL-1β (50 ng/ml) for 48 h. The production of soluble MICA on IL-1β-treated or non-treated normal hepatocytes was examined by specific ELISA. *ND* not detected

These results demonstrated that IL-1β could induce the increase in the production of soluble MICA only from HCC cells, but not from normal hepatocytes.

IL-1β treatment increases the production of soluble MICA from various cancer cells

We also examined IL-1β-dependent MICA regulation on another cancer cells including a gastric cancer cell line (MKN1), colon cancer cell lines (HCT116, HT29) and a cervical cancer cell line (HeLa). The expressions of membrane-bound MICA on these cells did not change by the addition of IL-1β in all cancer cells. Interestingly, the addition of IL-1β resulted in significant increase in the production of soluble MICA in all cancer cells (Fig. 3).

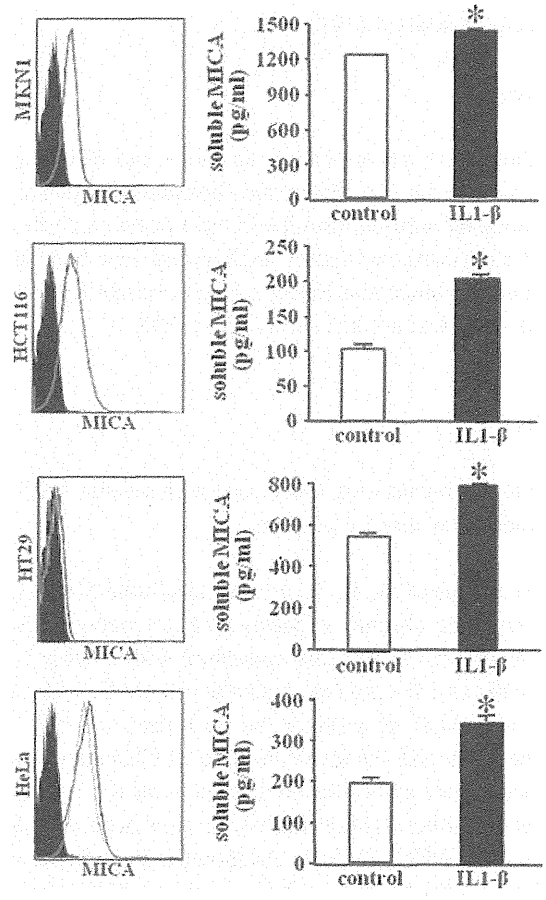

Fig. 3 Soluble MICA production of IL-1β-treated various cancer cells. Various cancer cells including MKN1, HCT116, HT29 and HeLa cells were treated in the presence or absence of IL-1β (50 ng/ml) for 48 h. Soluble MICA production of IL-1β-treated or non-treated various cancer cells was evaluated by specific ELISA (*right panel*). sMICA, soluble MICA. We also examined the expression of membrane-bound MICA on IL-1β-treated or non-treated various cancer cells by flow cytometry (*left panel*). *Black line histograms*, MICA staining of non-treated cells; *Gray line histograms*, MICA staining of IL-1β-treated cells; *shaded/black histograms*, control IgG isotype Ab staining. Similar results were obtained from two independent experiments. $*p < 0.05$

These results demonstrated that IL-1β could induce the increase in the production of soluble MICA not only from HCC cells but also from various cancer cells.

ADAM9 activated by IL-1β plays important roles in the production of soluble MICA from HCC cells

We next examined the mRNA of MICA and the production of soluble MICA in HCC cells treated with various doses of IL-1β. As shown in Fig. 4a, mRNA expression of MICA in IL-1β-treated PLC/PRF/5 cells significantly increased but that in HepG2 cells did not. The production of soluble MICA in IL-1β-treated PLC/PRF/5 cells significantly increased in a dose-dependent manner, and the production of soluble MICA significantly increased in 50 ng/ml IL-1β-treated HepG2 cells. Recently, members of the metzincin superfamily, such as ADAM proteins, have been reported to play essential roles in the proteolytic release of the ectodomain of transmembranous proteins, including MICA, from the cell surface [17, 20]. We previously reported that ADAM9 plays essential roles in MICA shedding in human HCC cells and that the activation of ADAM9 protease resulted in up-regulation of the production of soluble MICA from human HCC cells [19]. So we examined the involvement of ADAM9 in the up-regulation of soluble MICA production in IL-1β-treated HCC cells. As shown in Fig. 4b, mRNA levels of ADAM9 in IL-1β-treated PLC/PRF/5 cells significantly increased in a dose-dependent manner. mRNA of ADAM9 in IL-1β-treated HepG2 cells significantly increased in 10 ng/ml and 50 ng/ml IL-1β-treated HepG2 cells. The ADAM9 protein expression including both pro-form and active form also increased in IL-1β-treated HCC cells (Fig. 4c). To confirm the involvement of ADAM9 in IL-1β-treated HCC cells, we examined the soluble MICA production in IL-1β-treated ADAM9-knockdown (ADAM9KD) HCC cells. Both PLC/PRF/5 and HepG2 cells were transfected with ADAM9-siRNA or an irrelevant siRNA as a control. The expression of ADAM9 was clearly suppressed in PLC/PRF/5 cells and HepG2 cells at protein levels (Fig. 5a). In both PLC/PRF/5 and HepG2 cells transfected with control siRNA, the productions of soluble MICA in IL-1β-treated cells were significantly higher than those in non-treated HCC cells. In contrast, the production of soluble MICA in IL-1β-treated ADAM9KD-HepG2 cells was similar to that in non-treated ADAM9KD-HepG2 cells (Fig. 5b). The production of soluble MICA in IL-1β-treated ADAM9KD-PLC/PRF/5 cells also tended to decrease compared with that in non-treated ADAM9KD-PLC/PRF/5 cells (Fig. 5b). The decrease in soluble MICA production in ADAM9KD cells was different between PLC/PRF/5 cells and HepG2 cells. However, these results suggested at least that the increase in ADAM9 expression by IL-1β resulted in the increase in soluble MICA levels in IL-1β-treated HCC cells.

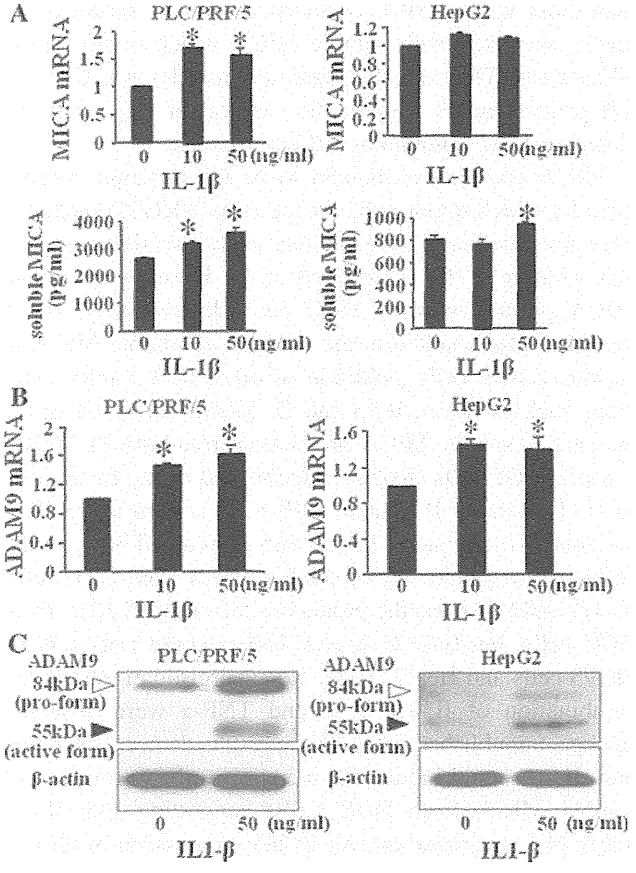

Fig. 4 IL-1β increased the ADAM9 expression of HCC cells and the production of soluble MICA. PLC/PRF/5 and HepG2 cells were cultured with 0, 10 and 50 ng/ml IL-1β for 48 h. **a** The production of soluble MICA from IL-1β-treated HCC cells was examined by specific ELISA, and mRNA levels of MICA of IL-1β-treated HCC cells were examined by real-time PCR. **b**, **c** mRNA and protein expression of ADAM9 by real-time RT-PCR (**b**) and western blotting (**c**), respectively. Representative results are shown. Similar results were obtained from 3 independent experiments. *$p < 0.05$

IL-1β-treated HCC cells are resistant to the cytolytic activity of NK cells

We next examined whether IL-1β could modify the NK sensitivity of human HCC cells. The cytolytic activities of NK cells against IL-1β-treated PLC/PRF/5 and IL-1β-treated HepG2 cells were lower than those against non-treated HCC cells (Fig. 5c). These results demonstrated that IL-1β treatment resulted in the increased resistance of HCC cells to NK cells.

Discussion

The liver contains a large compartment of innate immune cells (NK cells and NKT cells) and acquired immune cells

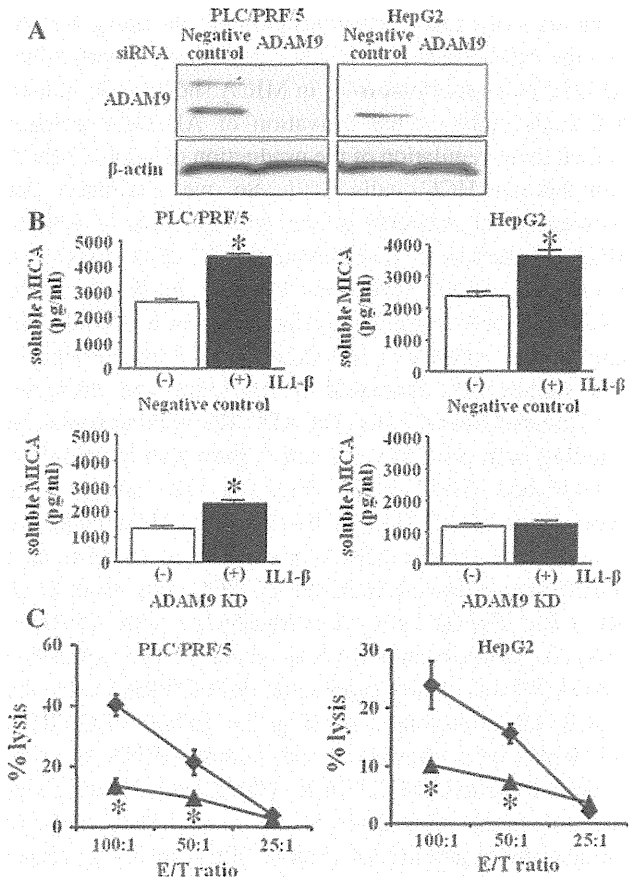

Fig. 5 The production of soluble MICA of ADAM9KD-HCC cells and the cytolytic activity against IL-1β-treated HCC cells. **a** Both HCC cells (PLC/PRF/5 and HepG2) were transfected with ADAM9 siRNA (ADAM9KD) or an irrelevant siRNA (negative control), and at 24-h post-transfection, the protein expression of ADAM9 was examined by western blotting. **b** Both HCC cells were cultured with (+) or without (−) 50 ng/ml IL-1β for 48 h. Soluble MICA production from ADAM9KD-HCC cells or negative control-HCC cells was evaluated by specific ELISA. *$p < 0.05$. Similar results were obtained from 3 independent experiments. **c** Both PLC/PRF/5 and HepG2 cells were cultured with or without IL-1β (50 ng/ml) for 48 h. The cytolytic activities of NK cells against IL-1β-treated or non-treated PLC/PRF/5 and HepG2 cells were evaluated by ^{51}Cr-releasing assay. Non-treated cells (*filled diamond*), IL-1β-treated cells (*filled triangle*). Representative results are shown. Similar results were obtained from three independent experiments. *$p < 0.05$ versus the cytolytic activity of non-treated cells. Similar results were obtained from 3 independent experiments

(T cells) [21, 22]. Recent study has demonstrated that innate immune system via NKG2D signal, expressing on NK cells, might play critical roles in tumor surveillance [23]. However, the escape mechanism of HCC cells from NK cells remains unclear. We previously demonstrated that membrane-bound MICA, activating molecule of NK cells, on HCC cells plays essential roles in the NK sensitivity of HCC cells [13, 24] and that the serum soluble MICA increase along the progression of chronic liver disease [18]. The production of soluble MICA in HCC patients is the highest compared with chronic hepatitis or liver cirrhosis patients without HCC [18]. These results suggest that unknown factors may accelerate the cleavage of MICA in HCC cells. IL-1β is produced mainly by local immune cells including activated Kupffer cells [25]. Because IL-1β increased in CH or LC patients [26–28], we focus on the possible role of IL-1β in the escape mechanism of HCC cells from NK cells.

Inflammatory cytokines including IL-1β and IL-6 increased in CH or LC patients [26–28], suggesting that both IL-1β and IL-6 might play roles in the HCC development. Recently high serum IL-6 level was an independent risk factor for HCC development in both chronic hepatitis C and B patients [29, 30], which suggested the possible roles of IL-6 in HCC development. However, the IL-1β levels in chronic liver disease, premalignant conditions, have been little reported. In this study, we demonstrated that serum IL-1β levels in chronic hepatitis C patients with HCC occurrence were significantly higher than those without HCC occurrence and that serum IL-1β levels correlated with soluble MICA which could inhibit NK activity. These results suggested that elevated IL-1β in CH patients might support the survival of HCC cells by changing local immunological environment.

MICA shedding is thought to be the principle mechanism by which tumor cells escape from NKG2D-mediated immunosurveillance [16]. In this study, we demonstrated that addition of IL-1β resulted in the increase in soluble MICA production from HCC cells. Interestingly, IL-1β treatment also resulted in the increase of soluble MICA in various cancer cells. Addition of other IL-1 family cytokines such as IL-1α, Il-18 and IL-33 did not result in the increase in soluble MICA production from both PLC/PRF/5 and HepG2 cells (Kohga, unpublished data). In addition to IL-1β, serum IL-6 and TNF-α are elevated in HCC patients. We compared IL-1β with IL-6 and TNF-α in the ability of the production of soluble MICA from HCC cells. IL-1β could increase the production of soluble MICA from HCC cells, but both IL-6 and TNF-α could not in PLC/PRF/5 cells and HepG2 cells. No synergistic effects of the combination of IL-1β, IL-6 and TNF-α were observed (Kohga, unpublished data). These results demonstrated that only IL-1β could induce the increase in the production of soluble MICA from HCC cells, suggesting that IL-1β might play an important role in the progression of HCC.

IL-1β treatment resulted in the increase in soluble MICA production but not the increase of mRNA in HepG2 cells. The production of soluble MICA depended on both the production of mRNA and the shedding of ADAM9. We previously demonstrated that ADAM9 plays an essential role in the shedding of MICA in HCC cells [19]. In the present study, we demonstrated that IL-1β treatment resulted in the increase in ADAM9 expression in HepG2

cells and that ADAM9 knockdown by siRNA resulted in the decrease in the production of soluble MICA from IL-1β-treated HepG2 cells. Our results suggested at least that the increase in ADAM9 might resulted in the increase in the shedding of soluble MICA in the IL-1β-treated HCC cells.

Recent studies have identified various metalloproteinases responsible for MICA/B cleavage in various cancers [31]. We previously found that ADAM9 plays critical roles in the shedding of MICA in human HCC. ADAM9 was directly associated with decreasing the expression of membrane-bound MICA and increasing the production of soluble MICA in human HCC [19]. Thus, it would be interesting to examine the activity of ADAM9 in IL-1β-treated HCC cells to understand how IL-1β regulates the production of soluble MICA from HCC cells. We demonstrated that IL-1β treatment could increase the mRNA and protein expression of ADAM9 in HCC cells and that ADAM9 knockdown in HCC cells resulted in decreasing of the soluble MICA production. These results suggested that ADAM9 played an important role in the increase in soluble MICA production from IL-1β-treated HCC cells. Both ADAMs and ADAMs with thrombospondin motifs (ADAMTS) are proteinases closely related to matrix metalloproteinases (MMPs). Structure of ADAMs and ADAMTS is highly conserved and involves metalloproteinase and disintegrin domains endowing them with features of both proteinases and adhesion molecules [32]. Several ADAMTSs including ADAMTS1 and ADAMTS9 were activated by IL-1β via NFATc1 transcription factor in chondrosarcoma [33, 34]. Although IL-1β may regulate such transcription factors in HCC cells, the detail mechanism of the activation of ADAM9 by IL-1β remains unclear. The concentration of IL-1β in our in vitro study was high compared with the serum IL-1β concentration level. However, the local IL-1β concentration in the liver tissues still remains unknown and may differ from the serum IL-1β concentration. Our in vitro study at least demonstrated that IL-1β could enhance the production of soluble MICA via up-regulating the expressions of ADAM9 in HCC cells, which might support the possible role of IL-1β in the survival of HCC cells.

Cai et al. [35] demonstrated that the numbers of CD56+ NK cells reduced in HCC tissues compared with healthy donors and CD56+ NK cells in HCC patients displayed impairments in cytotoxicity and IFN-γ production. This suggests that immunological microenvironment in liver tissues of CH patients might be favorable for the survival of HCC cells. We demonstrated that serum IL-1β levels correlated with soluble MICA in CH patients, which is consistent with our in vitro data. This suggests that the chronic elevation of IL-1β in CH patients might impair the function of NK cells by accelerating the production of soluble MICA. We also demonstrated that IL-1β treatment resulted in the inhibition of the cytolytic activity of NK cells against HCC cells. Intrahepatic activated macrophages and plasma cells could produce IL-1β inducing the inflammatory process in chronic liver disease [36]. If we could control the production of IL-1β with new reagents, it might be possible to develop a new therapeutic strategy against HCC. IL-1β receptor antagonist (IL-1RA) has been reported to apply clinically to the treatment of rheumatoid arthritis [37]. We believe the future clinical application of IL-1RA in HCC treatment as a new agent.

In spite of recent progress in the understanding of HCC, there remains to be unknown mechanism of the escape of HCC cells from innate immunity. We have shown here that ADAM9 was directly associated with increasing the production of soluble MICA in IL-1β-treated human HCC. These findings might indicate that IL-1β contributes to the survival of HCC cells by inhibiting innate immunity.

Acknowledgments This work was supported by a Grant-in-Aid from the Ministry of Education, Culture, Sports, Science and Technology of Japan and a Grant-in-Aid for Research on Hepatitis and BSE from the Ministry of Health, Labour and Welfare of Japan.

References

1. Dinarello CA (1996) Biologic basis for interleukin-1 in disease. Blood 87:2095–2147
2. Napoli J, Bishop GA, McGuinness PH, Painter DM, McCaughhan GW (1996) Progressive liver injury in chronic hepatitis C infection correlates with increased intrahepatic expression of Th1-associated cytokines. Hepatology 24:759–765
3. Powell EE, Edwards-Smith CJ, Hay JL, Clouston AD, Crawford DH, Shorthouse C, Purdie DM, Jonsson JR (2000) Host genetic factors influence disease progression in chronic hepatitis C. Hepatology 31:828–833
4. Tilg H, Wilmer A, Vogel W, Herold M, Nolchen B, Judmaier G, Huber C (1992) Serum levels of cytokines in chronic liver diseases. Gastroenterology 103:264–274
5. Bidwell J, Keen L, Gallagher G et al (1999) Cytokine gene polymorphism in human disease: on-line databases. Genes Immun 1:3–19
6. El-Omar EM, Carrington M, Chow WH et al (2000) Interleukin-1 polymorphisms associated with increased risk of gastric cancer. Nature 404:398–402
7. Howell WM, Calder PC, Grimble RF (2002) Gene polymorphism, inflammatory disease and cancer. Proc Nutr Soc 61:447–456
8. Wang Y, Kato N, Hoshida Y et al (2003) Interleukin-1β gene polymorphism associated with hepatocellular carcinoma in hepatitis C virus infection. Hepatology 37:65–71
9. Tanaka Y, Furuta T, Suzuki S, Orito E, Yeo AE, Hirashima N, Sugauchi F, Ueda R, Mizokami M (2003) Impact of interleukin-1β genetic polymorphism on the development of hepatitis C virus-related hepatocellular carcinoma in Japan. J Infec Dis 187:1822–1825
10. Hirankarn N, Kimkong I, Kummee P, Tangkijvanich P, Poovorawan Y (2006) Interleukin-1β gene polymorphism associated with hepatocellular carcinoma in hepatitis B virus infection. World J Gastroenterol 12:776–779

11. Tu S, Bhagat G, Cui G, Takaishi S, Kurt-Jones EA, Rickman B, Betz KS, Penz-Oesterreicher M, Bjorkdahl O, Fox JG, Wang TC (2008) Overexpression of interleukin-1β induces gastric inflammation and cancer and mobilizes myeloid-derived suppressor cells in mice. Cancer Cell 14:408–419
12. Groh V, Rhinehart R, Secrist H, Bauer S, Grabstein KH, Spies T (1999) Broad tumor-associated expression and recognition by tumor-derived $\gamma\delta$T cells of MICA and MICB. Proc Natl Acad Sci USA 96:6879–6884
13. Jinushi M, Takehara T, Tatsumi T et al (2003) Expression of MICA and MICB in human hepatocellular carcinomas and their regulation by retinoic acids. Int J Cancer 104:354–361
14. Ogasawara K, Lanier LL (2005) NKG2D in NK and T cell-mediated immunity. J Clin Immunol 25:534–540
15. Caudert JD, Held W (2006) The role of the NKG2D receptor for tumor immunity. Semin Cancer Biol 16:333–343
16. Groh V, Wu J, Yee C, Spies T (2002) Tumor-derived soluble MIC ligands impair expression of NKG2D and T cell activation. Nature 419:734–738
17. Salih HR, Rammensee HG, Steinle A (2002) Downregulation of MICA on human tumors by proteolytic shedding. J Immunol 169: 4098–4102
18. Kohga K, Takehara T, Tatsumi T et al (2008) Serum levels of soluble major histocompatibility complex (MHC) class I-related chain A in patients with chronic liver disease and changes during transcatheter arterial embolization for hepatocellular carcinoma. Cancer Sci 99:1643–1649
19. Kohga K, Takehara T, Tatsumi T, Ishida H, Miyagi T, Hosui A, Hayashi N (2010) Sorafenib inhibits the shedding of MICA on hepatocellular carcinoma cell by downregulating ADAM9. Hepatology 51:1264–1273
20. Holdenrieder S, Stieber P, Peterfi A, Nagel D, Steinle A, Salih HR (2006) Soluble MICA in malignant disease. Int J Cancer 118: 684–687
21. Doherty DG, O'Farrelly C (2000) Innate and adaptive lymphoid cells in human liver. Immunol Rev 174:5–20
22. Mehal WZ, Azzaroli F, Crispe IN (2001) Immunology of the healthy liver: old questions and new insights. Gatsroenterology 120:250–260
23. Guerra N, Tan YX, Joncker NT et al (2008) NKG2D-deficient mice are defective in tumor surveillance in models of spontaneous malignancy. Immunity 28:571–580
24. Kohga K, Takehara T, Tatsumi T, Miyagi T, Ishida H, Ohkawa K, Kanto T, Hiramatsu N, Hayashi N (2009) Anti-cancer chemotherapy inhibits MICA ectodomain shedding by downregulating ADAM10 expression in hepatocellular carcinoma. Cancer Res 69:8050–8057
25. Oyanagi Y, Takahashi T, Matsui S, Takahashi S, Boku S, Takahashi K, Furukawa K, Arai F, Asakura H (1999) Enhanced expression of interleukin-6 in chronic hepatitis C. Liver 19:464–472
26. Lapinski TW (2001) The levels of IL-1β, IL-4 and IL-6 in the serum and the liver tissue of chronic HCV-infected patients. Arch Immunol Ther Exp 49:311–316
27. Bortolami M, Kotsafti A, Cardin R, Farinati F (2008) Fas/FasL system, IL-1β expression and apoptosis in chronic HBV and HCV liver disease. J Viral Hepat 15:515–522
28. Migita K, Abiru S, Maeda Y et al (2005) Serum levels of interleukin-6 and its soluble receptors in patients with hepatitis C virus infection. Human Immunol 67:27–32
29. Nakagawa H, Maeda S, Yoshida H et al (2009) Serum IL-6 levels and the risk for hepatocarcinogenesis in chronic hepatitis C patients: an analysis based on gender difference. Int J Cancer 125:2264–2269
30. Wong VW, Yu J, Cheng AS et al (2009) High serum interleukin-6 level predicts future hepatocellular carcinoma development in patients with chronic hepatitis B. Int J Cancer 124:2766–2770
31. Waldhauer I, Goehlsdorf D, Gieseke F et al (2008) Tumor-associated MICA is shed by ADAM proteases. Cancer Res 68: 6368–6376
32. Seals DF, Courtneidge SA (2003) The ADAMs family of metalloproteases: multidomain proteins with multiple functions. Genes Dev 17:7–30
33. Yaykasli KO, Oohashi T, Hirohata S, Hatipoglu OF, Inagawa K, Demircan K, Ninomiya Y (2009) ADAMTS9 activation by interleukin 1 beta via NFATc1 in OUMS-27 chondrosarcoma cells and in human chondrocytes. Mol Cell Biochem 323:69–79
34. Kalinski T, Krueger S, Sel S, Wemer K, Ropke M, Roessner A (2007) ADAMTS1 is regulated by interleukin-1beta, not by hypoxia, in chondrosarcoma. Hum Pathol 38:86–94
35. Cai L, Zhang Z, Zhou L et al (2008) Functional impairment in circulating and intrahepatic NK cell and relative mechanism in hepatocellular carcinoma patients. Clin Immunol 129:428–437
36. Hassan G, Moreno S, Massimi M, Di Biagio P, Stefanini S (1997) Interleukin-1-producing plasma cells in close contact with hepatocytes in patients with chronic active hepatitis. J Hepatol 27:6–17
37. Gabby C, Lamacchia C, Palmer G (2010) IL-1 pathway in inflammation and human disease. Nat Rev Rheumatol 6:232–241

Research Article

EASL EUROPEAN ASSOCIATION FOR THE STUDY OF THE LIVER | JOURNAL OF HEPATOLOGY

Bak deficiency inhibits liver carcinogenesis: A causal link between apoptosis and carcinogenesis

Hayato Hikita[1], Takahiro Kodama[1], Satoshi Shimizu[1], Wei Li[1], Minoru Shigekawa[1], Satoshi Tanaka[1], Atsushi Hosui[1], Takuya Miyagi[1], Tomohide Tatsumi[1], Tatsuya Kanto[1], Naoki Hiramatsu[1], Eiichi Morii[2], Norio Hayashi[3], Tetsuo Takehara[1,*]

[1]*Department of Gastroenterology and Hepatology, Osaka University Graduate School of Medicine, Suita, Osaka 565-0871, Japan;*
[2]*Department of Pathology, Osaka University Graduate School of Medicine, Suita, Osaka 565-0871, Japan;*
[3]*Kansai-Rosai Hospital, Amagasaki, Hyogo 660-8511, Japan*

Background & Aims: Hepatocyte apoptosis is a key feature of chronic liver disease including viral hepatitis and steatohepatitis. A previous study demonstrated that absence of the Bcl-2 family protein Mcl-1 led to increased hepatocyte apoptosis and development of liver tumors in mice. Since Mcl-1 not only inhibits the mitochondrial pathway of apoptosis but can also inhibit cell cycle progression and promote DNA repair, it remains to be proven whether the tumor suppressive effects of Mcl-1 are mediated by prevention of apoptosis.

Methods: We examined liver tumor development, fibrogenesis, and oxidative stress in livers of hepatocyte-specific knockout (KO) of *Mcl-1* or *Bcl-xL*, another key antagonist of apoptosis in hepatocytes. We also examined the impact of additional KO of *Bak*, a downstream molecule of Mcl-1 towards apoptosis but not the cell cycle or DNA damage pathway, on tumor development, hepatocyte apoptosis, and inflammation.

Results: *Bcl-xL* KO led to a high incidence of liver tumors in 1.5-year-old mice, similar to *Mcl-1* KO. Bcl-xL- or Mcl-1-deficient livers showed higher levels of TNF-α production and oxidative stress than wild-type livers at as early as 6 weeks of age and oxidative DNA damage at 1.5 years. Deletion of Bak significantly inhibited hepatocyte apoptosis in *Mcl-1* KO mice and reduced the incidence of liver cancer, coinciding with reduction of TNF-α production, oxidative stress, and oxidative DNA damage in non-cancerous livers.

Conclusions: Our findings strongly suggest that chronically increased apoptosis in hepatocytes is carcinogenic and offer genetic evidence that inhibition of apoptosis may suppress liver carcinogenesis in chronic liver disease.

Keywords: Bcl-xL; Mcl-1; 8-OHdG.
Received 26 September 2011; received in revised form 19 January 2012; accepted 21 January 2012; available online 10 March 2012
* Corresponding author. Address: Department of Gastroenterology and Hepatology, Osaka University Graduate School of Medicine, 2-2 Yamada-oka, Suita, Osaka 565-0871, Japan. Tel.: +81 6 6879 3621; fax: +81 6 6879 3629.
E-mail address: takehara@gh.med.osaka-u.ac.jp (T. Takehara).
Abbreviations: HCC, hepatocellular carcinoma; ALT, alanine aminotransferase; RT-PCR, reverse-transcription PCR; HO-1, heme oxygenase-1; NQO1, NAD(P)H:quinone oxidoreductase 1; 8-OHdG, 8-hydroxy-2′-deoxyguanosine; TUNEL, terminal deoxynucleotidyl transferase-mediated deoxyuridine triphosphate nick-end labeling.

Introduction

Apoptosis of epithelial cells, as well as infiltration of inflammatory cells or deposits of fibers, is frequently observed in the chronic diseased liver, which is a high-risk condition for hepatocellular carcinoma (HCC) [1]. For example, Fas-mediated hepatocyte apoptosis is a mechanism of cell death in chronic hepatitis C virus infection and hepatitis B virus infection [2,3]. Hepatocyte apoptosis shows correlation with inflammation and fibrosis in non-alcoholic steatohepatitis [4]. Cytokeratin 18 neoepitope, a well-established marker of caspase activity in serum, is elevated and associated with liver injury in chronic viral hepatitis and non-alcoholic steatohepatitis [5–7]. Although viral factors and overt organ inflammation linked to liver cancer development have been extensively studied [8,9], less information is available on the involvement of hepatocyte apoptosis in liver cancer development.

Bcl-xL and Mcl-1 are among the anti-apoptotic members of the Bcl-2 family, which antagonizes the pro-apoptotic function of Bak and/or Bax at the mitochondrial outer membrane. We previously reported that hepatocyte-specific *Bcl-xL* or *Mcl-1* knockout (KO) mice showed persistent apoptosis of hepatocytes in the adult liver and mild fibrotic responses [10,11]. A very recent study by Weber *et al.* [12] demonstrated that hepatocyte-specific *Mcl-1* KO mice developed liver tumors in old age. This observation raised the important possibility that apoptosis in hepatocytes could lead to the development of liver cancer. However, as Mcl-1 has been reported to possess functions other than anti-apoptosis, such as cell cycle inhibition [13,14] and DNA damage repair [15,16], it is difficult to conclude that the phenotypes observed in *Mcl-1* KO are simply ascribable to apoptosis. Indeed, *Mcl-1* KO mice showed not only increased apoptosis but also increased regeneration in the liver [12]. In the present study, we demonstrated that hepatocyte-specific *Bcl-xL* KO mice also develop liver cancer in old age and that deficiency of Bak, a downstream effector molecule of Mcl-1 towards the

Table 1. Incidence of liver tumors in KO mice.

Age (yr)	Genotype	Tumor incidence
1.5		
	Bcl-xL$^{+/+}$	0% (0/10)
	Bcl-xL$^{-/-}$	88% (7/8)*
1		
	Bcl-xL$^{+/+}$	0% (0/4)
	Bcl-xL$^{-/-}$	27% (3/11)
1.5		
	Mcl-1$^{+/+}$	0% (0/22)
	Mcl-1$^{-/-}$	100% (16/16)*
1		
	Mcl-1$^{-/-}$ *Bak*$^{+/+}$	64% (14/22)
	Mcl-1$^{-/-}$ *Bak*$^{-/-}$	0% (0/7)*

*p <0.05 *vs.* control.

mitochondrial pathway of apoptosis, clearly suppresses hepatocyte apoptosis and liver carcinogenesis in *Mcl-1* KO mice. We also considered possible mechanisms involving oxidative stress that underlie elevated malignant transformation in the apoptosis-prone liver. The present study offers strong support for the hypothesis that chronically increased apoptosis in hepatocytes is carcinogenic. It also provides genetic evidence that inhibition of apoptosis may suppress liver carcinogenesis in chronic liver disease.

Materials and methods

Mice

Conditional *Bcl-xL* KO mice (*bcl-x*$^{flox/flox}$ *Alb-Cre*) and *Mcl-1* KO mice (*mcl-1*$^{flox/flox}$ *Alb-Cre*) were previously described [11]. We purchased *Bak* KO mice (*bak*$^{-/-}$) from the Jackson Laboratory (Bar Harbor, ME). We generated hepatocyte-specific Bak/Mcl-1 double KO mice (*bak*$^{-/-}$ *mcl-1*$^{flox/flox}$ *Alb-Cre*) by mating the strains. They were maintained in a specific pathogen-free facility and treated with humane care with approval from the Animal Care and Use Committee of Osaka University Medical School. Measurement of serum alanine aminotransferase (ALT) level, caspase-3/7 activity and histological analyses have been previously described [11].

Western blot analysis

For immunodetection, the following antibodies were used: anti-Bcl-xL antibody (Santa Cruz Biotechnology, Santa Cruz, CA), anti-Mcl-1 antibody (Rockland, Gilbertsville, PA), anti-Bak antibody (Millipore, Billerica, MA), anti-Bax antibody, anti-ERK antibody, anti-phospho-ERK antibody, anti-p38 antibody, anti-phospho-p38 antibody, anti-JNK antibody, anti-phospho-JNK antibody, anti-PCNA antibody (Cell Signaling Technology, Danvers, MA), and anti-beta-actin antibody (Sigma–Aldrich, Saint Louis, MO).

Real-time reverse-transcription PCR (RT-PCR)

The following TaqMan Gene Expression Assays (Applied Biosystems, Foster City, CA) were used: mouse-AFP (Mm00431715_m1), mouse-glypican-3 (Mm00516722_m1), mouse-IL-6 (Mm00446190_m1), mouse-TNF-α (Mm00443258_m1), mouse-MCP-1 (Mm00441242_m1), mouse-CD68 (Mm03047343_m1), mouse-CD4 (Mm00442754_m1), mouse-CD8 (Mm01182108_m1), mouse-heme oxygenase-1 (HO-1) (Mm00516005_m1), mouse-NAD(P)H:quinone oxidoreductase 1 (NQO1) (Mm00500821_m1), and mouse-Beta actin (Mm00607939_s1). All expression levels were corrected with the quantified expression level of beta actin.

Immunohistochemistry

8-Hydroxy-2′-deoxyguanosine (8-OHdG), cleaved caspase-9, PCNA, and ki-67 were labeled in paraffin-embedded liver sections using anti-8-OHdG antibody (Nikken Seil, Tokyo, Japan), anti-cleaved caspase-9 antibody, anti-PCNA antibody (Cell Signaling Technology), and anti-ki-67 antibody (Dako, Tokyo, Japan), respectively. Terminal deoxynucleotidyl transferase-mediated deoxyuridine triphosphate nick-end labeling (TUNEL) was performed according to a previously reported procedure [17].

Statistical analysis

Data are presented as mean ± SD. Differences between two groups were determined using the Student's *t*-test for unpaired observations. Carcinogenesis rates were analyzed using the Chi-square test. Multiple comparisons of *Bak/Mcl-1* double KO mice were performed by ANOVA followed by Scheffe *post hoc* correction. Fisher *post hoc* correction was used for the other multiple comparisons. A p <0.05 was considered statistically significant.

Results

Bcl-xL KO mice develop liver tumors in old age

We previously reported that hepatocyte-specific *Bcl-xL* KO mice developed spontaneous hepatocyte apoptosis by the mitochondrial pathway (Supplementary Fig. 1A) at as early as 1 month of age with a gradual increase in the liver fibrotic response from 3 to 7 months [10]. To examine the phenotypes at later time points, we sacrificed *Bcl-xL* KO mice and their control littermates at 1 and 1.5 years of age. Macroscopic tumors had developed in the liver of 27% and 88% of the KO mice, respectively, but not in the control littermates (Fig. 1A and Table 1). Most of the *Bcl-xL* KO mice had multiple tumors and the liver body-weight ratio for *Bcl-xL* KO mice was significantly higher than that of the control mice (Fig. 1B and C). Tumors were histologically defined as well-differentiated HCCs (Fig. 1D). To find out whether the *bcl-x* gene is really targeted in the tumors, we performed Western blot analysis for the expression of the Bcl-2 family proteins (Fig. 1E and Supplementary Fig. 2A). The tumors were confirmed to be deficient for Bcl-xL, excluding the possibility that transformed cells arising from hepatocytes in which the *bcl-x* gene was not deleted had expanded to form tumors. Interestingly, most of these tumors showed apparently higher levels of Mcl-1 expression than the wild-type liver or the non-cancerous surrounding tissues. Reciprocal overexpression of Mcl-1 may explain the possible survival advantage of these tumors. Tumors in *Bcl-xL* KO mice expressed higher levels of α-fetoprotein (Fig. 1F) and frequently showed activation of ERK and JNK (Fig. 1G), which are observed in human HCC [18,19].

Liver tumors in Mcl-1 KO mice show similar characteristics to human HCC

We have previously reported phenotypes of hepatocyte-specific *Mcl-1* KO mice, which display spontaneous hepatocyte apoptosis by the mitochondrial pathway (Supplementary Fig. 1B) and liver fibrotic responses at an early age [11]. Since our *Mcl-1* floxed mice differed from those of Weber *et al.* [12] in origin, we next examined the development of liver tumors in our hepatocyte-specific *Mcl-1* KO mice. All the *Mcl-1* KO mice, but none of the control littermates, developed liver tumors at 1.5 years of age, with a significant increase of liver body-weight ratio (Fig. 2A–C

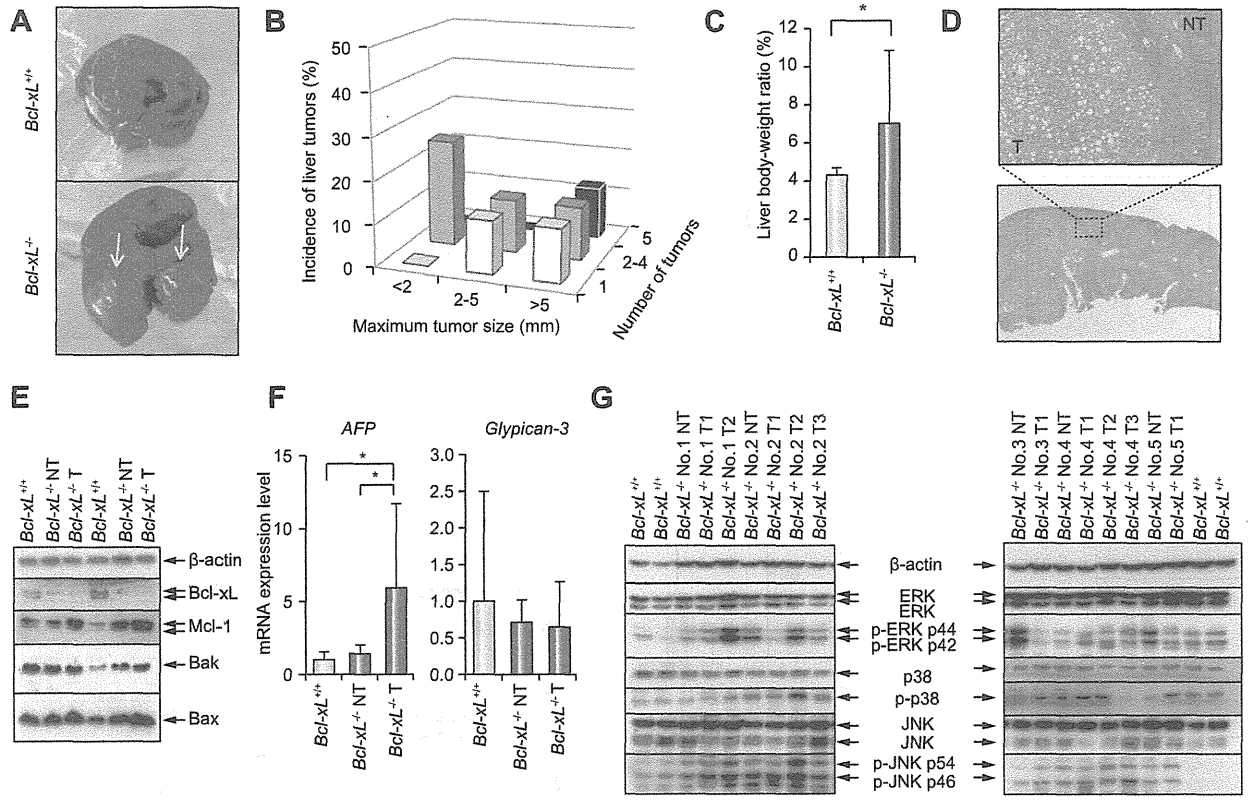

Fig. 1. Liver tumors in *Bcl-xL* KO mice. (A–E) Hepatocyte-specific *Bcl-xL*-deficient mice (*Bcl-xL*$^{-/-}$) (N = 8) and their control littermates (*Bcl-xL*$^{+/+}$) (N = 10) were sacrificed at 1.5 years of age. (A) Representative macroscopic view of the livers with arrows indicating tumors. (B) Incidence of liver tumors separated by maximum tumor size and number of tumors. (C) Liver body-weight ratio. (D) Representative histology of liver tumors in *Bcl-xL* KO mice. (E) Western blot of the Bcl-2 family proteins in tumors (T) and surrounding non-cancerous livers (NT) of *Bcl-xL* KO mice and livers of control mice. (F and G) Characteristics of liver tumors in *Bcl-xL* KO mice. (F) Real-time RT-PCR analysis of the expression levels of α-fetoprotein (*AFP*) and *glypican-3* mRNA (N = 9 or 10 per group). (G) Expression and activation of mitogen-activated protein kinases. *p <0.05.

and Table 1). As in the case of tumors of *Bcl-xL* KO mice, liver tumors that developed in *Mcl-1* KO mice were deficient for Mcl-1 expression and, in most cases, reciprocally overexpressed Bcl-xL (Fig. 2E and Supplementary Fig. 2B). These tumors expressed higher levels of α-fetoprotein and glypican-3 (Fig. 2F) and frequently showed activation of ERK and JNK (Fig. 2G).

Inflammatory response and oxidative stress occur in Bcl-xL- or Mcl-1-KO livers

To examine the molecular mechanism of tumor development, we examined gene expression in the livers of 6-week-old *Bcl-xL* or *Mcl-1* KO mice. Real-time RT-PCR analysis revealed increases of inflammatory cytokine TNF-α, but not IL-6, and chemokine MCP-1 in *Bcl-xL* and *Mcl-1* KO livers (Fig. 3A and B), despite overt histological inflammation (data not shown). Together with an increase of MCP-1, CD68 expression was significantly higher in KO livers than in control livers (Fig. 3C and D). In contrast, there was no difference in the expression of CD4 and CD8 between the groups. These findings suggest that activation or infiltration of myeloid-derived cells and production of TNF-α are characteristic of the *Bcl-xL* or *Mcl-1* KO liver. Together with the previous study reporting that TNF-α promotes cellular transformation [20], these results suggest that the increase in TNF-α may be one of the mechanisms of tumor development.

Since oxidative stress is also reported to cause carcinogenesis [21], we examined the expression of HO-1 and NQO1, inducible anti-oxidant enzymes, and 8-OHdG in the liver tissues. Real-time RT-PCR analysis revealed that HO-1 and NQO-1 expressions were significantly increased in *Mcl-1* KO livers at 6 weeks (Fig. 3E). 8-OHdG staining revealed that there were few 8-OHdG positive nuclei in both *Mcl-1* KO and the control liver at 6 weeks of age. However, scattered positive nuclei were observed in KO livers at 1.5 years of age, but not in the tumors, and the number of positive nuclei was significantly higher in KO livers than in control livers (Fig. 3F and Supplementary Fig. 3). Similarly, the number of 8-OHdG positive nuclei was significantly higher in *Bcl-xL* KO livers at 1.5 years of age than in control livers (Fig. 3G). These results suggest that oxidative stress may occur at as early as 6 weeks of age in KO livers and that oxidative injury arises at a later time point.

Bak deficiency significantly ameliorates hepatocyte apoptosis and reduces tumor development in Mcl-1 KO mice

Bak is a proapoptotic Bcl-2 family protein, which is able to oligmerize to form pores at the outer membrane of mitochondria. To understand whether inhibition of apoptosis could reduce the carcinogenic potential, we crossed *Mcl-1* KO mice and *Bak* KO mice and generated *Bak Mcl-1* double KO mice. As expected, *Bak* KO significantly suppressed hepatocyte apoptosis in *Mcl-1*